

การศึกษาปริมาณรังสีที่ผู้ป่วย แพทย์และเจ้าหน้าที่ได้รับ  
จากการส่องกล้องตรวจรักษาท่อทางเดินน้ำดีและตับอ่อน



นายฉัตรพงศ์ สุวรรณบุญฤทธิ์

ศูนย์วิทยุทรัพยากร  
จุฬาลงกรณ์มหาวิทยาลัย  
วิทยานิพนธ์นี้เป็นส่วนหนึ่งของการศึกษาตามหลักสูตรปริญญาวิทยาศาสตรมหาบัณฑิต

สาขาวิชาฉายาเวชศาสตร์ ภาควิหารังสีวิทยา

คณะแพทยศาสตร์ จุฬาลงกรณ์มหาวิทยาลัย

ปีการศึกษา 2552

ลิขสิทธิ์ของจุฬาลงกรณ์มหาวิทยาลัย

**RADIATION DOSE TO PATIENTS AND MEDICAL STAFF  
DURING ENDOSCOPIC RETROGRADE  
CHOLANGIOPANCREATOGRAPHY (ERCP) PROCEDURE**

**Mr.Wachirapong Suwanboonrit**



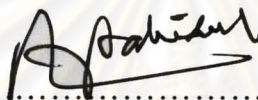
ศูนย์วิทยุทรัพยากร  
จุฬาลงกรณ์มหาวิทยาลัย

**A Thesis Submitted in Partial Fulfillment of the Requirements  
for the Degree of Master of Science Program in Medical Imaging  
Department of Radiology  
Faculty of Medicine  
Chulalongkorn University  
Academic Year 2009  
Copyright of Chulalongkorn University**

Thesis Title                    RADIATION DOSE TO PATIENTS AND  
MEDICAL STAFF DURING ENDOSCOPIC  
RETROGRADE  
CHOLANGIOPANCREATOGRAPHY    (ERCP)  
PROCEDURE  
By                                    Mr. Wachirapong Suwanboonrit  
Field of Study                    Medical Imaging  
Thesis Advisor                   Associate Professor Anchali Krisanachinda, Ph.D.  
Thesis Co-advisor              Associate Professor Rangsan Rerknimitr, M.D.

---

Accepted by the Faculty of Medicine, Chulalongkorn University in  
Partial Fulfillment of the Requirements for the Master's Degree

  
.....Dean of the Faculty of Medicine  
(Professor Adisorn Patradul, M.D.)

#### THESIS COMMITTEE

.....*Sivalee Suriyapee*.....Chairman  
(Associate Professor Sivalee Suriyapee, M.Eng.)

.....*Anchali*.....Thesis Advisor  
(Associate Professor Anchali Krisanachinda, Ph.D.)

.....*Rangsan Rerknimitr*..... Thesis Co-advisor  
(Associate Professor Rangsan Rerknimitr, M.D.)

.....*Franco Milano*.....External Examiner  
(Professor Franco Milano, Ph.D.)

วชิรพงศ์ สุวรรณบุญฤทธิ์ : การศึกษาปริมาณรังสีที่ผู้ป่วย แพทย์และเจ้าหน้าที่ได้รับ จากการส่องกล้องตรวจรักษาต่อทางเดินน้ำดีและตับอ่อน (RADIATION DOSE TO PATIENTS AND MEDICAL STAFF DURING ENDOSCOPIC RETROGRADE CHOLANGIOPANCREATOGRAPHY (ERCP) PROCEDURE)

อ.ที่ปรึกษาวิทยานิพนธ์หลัก: รศ.ดร. อัญชลี กฤษณจินดา

อ.ที่ปรึกษาวิทยานิพนธ์ร่วม: รศ.นพ. รังสรรค์ ฤกษ์นิมิตร ; 58 หน้า.

การศึกษานี้เป็นการวัดปริมาณรังสีที่ผิวของแพทย์ ในระหว่างการส่องกล้องตรวจรักษาต่อทางเดินน้ำดีและตับอ่อน โดยใช้เครื่องวัดรังสีชนิดเทอร์โมลูมิเนสเซนส์ (ทีแอลดี) รวมทั้งเป็นการหาความสัมพันธ์ระหว่างปริมาณรังสีที่ผิวของแพทย์กับปริมาณรังสีที่ผู้ป่วยได้รับซึ่งวัดได้โดยเครื่องแคปมิเตอร์

การศึกษานี้มีการเก็บข้อมูลทั้งหมดจากผู้ป่วย 40 ราย จากการส่องกล้องตรวจรักษาต่อทางเดินน้ำดีและตับอ่อน ในหน่วยเอกซเรย์หลอดเลือดและรังสีร่วมรักษา ฝ่ายรังสีวิทยา โรงพยาบาลจุฬาลงกรณ์ สภากาชาดไทย โดยแบ่งผู้ป่วยเป็น 2 ลักษณะ คือ ท่านอนคว่ำ 20 ราย และท่านอนตะแคงซ้าย 20 รายในงานบริการทางรังสีร่วมรักษา และใช้เครื่องเอกซเรย์เครื่องเดียวกัน เครื่องวัดรังสีทีแอลดีจะถูกติดตั้งบริเวณผิวของแพทย์ 5 ตำแหน่งต่อคน ปริมาณรังสีที่ผู้ป่วยได้รับวัดจากเครื่องแคปมิเตอร์ ซึ่งติดกับคอลลิเมเตอร์ของหลอดเลือดเอกซเรย์ และได้ศึกษาความสัมพันธ์ของปริมาณรังสีที่แพทย์ได้รับที่ผิวกับปริมาณรังสีที่ผู้ป่วยได้รับในแต่ละท่า

ผลของการศึกษาแสดงว่า ปริมาณรังสีที่ผิวสูงสุดที่แขนซ้ายของแพทย์มีค่า 244.02 ไมโครเกรย์ จากผู้ป่วยที่นอนตะแคงซ้าย และ 131.09 ไมโครเกรย์ จากผู้ป่วยที่นอนคว่ำ ซึ่งปริมาณรังสีสูงสุดที่ผิวของผู้ป่วยได้รับจากท่านอนตะแคงซ้ายมีค่า 124.06 มิลลิเกรย์ และ 82.93 มิลลิเกรย์จากท่านอนคว่ำ ซึ่งมีความแตกต่างกันอย่างมีนัยสำคัญทางสถิติ ปริมาณรังสีที่ผู้ป่วย แพทย์และเจ้าหน้าที่ได้รับมีความสัมพันธ์กันดังนี้ อัตราส่วนระหว่างปริมาณรังสีที่ผิวสูงสุดที่แขนซ้ายของแพทย์ต่อปริมาณรังสีจากผู้ป่วยที่นอนตะแคงซ้าย คือ 111.66 ไมโครเกรย์ ต่อ 10 เกรย์ตารางเซนติเมตร และอัตราส่วนระหว่างปริมาณรังสีที่ผิวดำสุดที่ช่องท้องส่วนล่างของแพทย์ต่อปริมาณรังสีจากผู้ป่วยที่นอนคว่ำ คือ 7.53 ไมโครเกรย์ ต่อ 10 เกรย์ตารางเซนติเมตร นอกจากความสัมพันธ์นี้ทำให้ทราบถึงการเพิ่มขึ้นของปริมาณรังสีจากเทคนิคการตรวจที่ต่างกันและจากความสัมพันธ์นี้จะได้นำไปพิจารณาจัดหาอุปกรณ์กำบังรังสีที่เหมาะสม เพื่อหลีกเลี่ยงการรับรังสีที่ไม่จำเป็น

ศูนย์วิทยทรัพยากร  
จุฬาลงกรณ์มหาวิทยาลัย

ภาควิชา.....รังสีวิทยา.....ลายมือชื่อนิติ.....จวิรพงศ์ สุวรรณบุญฤทธิ์.....

สาขาวิชา.....ฉายาเวชศาสตร์.....ลายมือชื่อ.ที่ปรึกษาวิทยานิพนธ์หลัก.....



ปีการศึกษา.....2552.....ลายมือชื่อ.ที่ปรึกษาวิทยานิพนธ์ร่วม.....



## 5174818830: MAJOR MEDICAL IMAGING

**KEYWORDS:** THERMOLUMINESCENT DOSIMETER / DOSE-AREA PRODUCT/ENDOSCOPIC RETROGRADE CHOLANGIOPANCREATOGRAPHY  
**WACHIRAPONG SUWANBOONRIT:** RADIATION DOSE TO PATIENTS AND MEDICAL STAFF DURING ENDOSCOPIC RETROGRADE CHOLANGIOPANCREATOGRAPHY (ERCP) PROCEDURE. THESIS ADVISOR: ASSOC. PROF. ANCHALI KRISANACHINDA, CO- ADVISOR: ASSOC. PROF. RANGSAN RERKNIMITR, 58 pp.

The objective of this study is to evaluate the radiation dose to patient at two positions (prone and left lateral) and to medical staff during ERCP procedure using dose area product (DAP) meter and thermoluminescent dosimeter (TLD). Data were recorded on 20 patients at prone position and 20 patients at left lateral position. The radiographic-fluoroscopic system manufactured by Siemens Model Polystar was used for ERCP procedure at King Chulalongkorn Memorial Hospital. Dose Area Product (DAP) manufactured by PTW Model Diamentor E, a transmission ionization chamber was attached to X-ray collimator to record the dose-area ( $\text{cGy}\cdot\text{cm}^2$ ) in order to determine the entrance surface air kerma (ESAK, mGy) of the patients at two positions (prone and left lateral) while the Kodak Portal Pack for localization imaging was placed on the patient's couch to determine the exposed area ( $\text{cm}^2$ ) on the surface of the patient. TLD was attached at five positions, left eye, thyroid, left forearm, lower abdomen and left leg of the medical staff during ERCP procedure. The average patient skin dose from DAP was higher at left lateral position of 124.06 (23.3-229.3) mGy than 82.93 (39.76-174.74) mGy at prone position. The medical staff received the maximum dose per procedure at the left forearm of 244.02 (54.79-1628.66)  $\mu\text{Gy}$  for patient at left lateral position and 131.09 (29.9-382.81)  $\mu\text{Gy}$  at prone position. The average surface dose the patient received during ERCP procedure at prone and lateral positions were 82.93 and 124.06 mGy per procedure which were significantly different. The medical staff also received higher dose at left lateral position than at prone position, but they were adequately protected from the risk of working with the radiation. The relation between medical staff and patient doses was established. The highest ratio between average medical staff doses and dose-area product is the left forearm and the lowest ratio is the lower abdomen of ERCP procedure. The highest ratio is 111.66  $\mu\text{Gy} / 10 \text{ Gy}\cdot\text{cm}^2$  and the lowest ratio is 7.53  $\mu\text{Gy} / 10 \text{ Gy}\cdot\text{cm}^2$ . The medical staff dose can be estimated from the patient dose using DAP method. This will help the medical staff to avoid the excess dose during their work.

Department ..... Radiology ..... Student's signature Wachirapong Suwanboonrit  
 Field of study ..... Medical Imaging ..... Advisor's signature   
 Academic Year ..... 2009 ..... Co-Advisor's signature 

## ACKNOWLEDGEMENTS

The success of this thesis could be attributed to the extensive support and assistance from my major advisor, Assoc. Prof. Dr. Anchali Krisanachinda and my co-advisor, Assoc. Prof. Dr. Rangsan Rerknimitr. I deeply thank for their valuable advice and guidance in this research.

I wish to thank my thesis committee, Assoc. Prof. Sivalee Suriyapee, Assoc. Prof. Dr. Anchali Krisanachinda, Department of Radiology, Assoc. Prof. Dr. Rangsan Rerknimitr, Department of Medicine, Faculty of Medicine, Chulalongkorn University and Professor Franco Milano, Florence University, Italy, for their kindness, helpful and valuable suggestion.

I would like to thank Mr.Sornjarod Oonsiri and Miss Puntiva Insang, Division of Radiation Oncology, Department of Radiology, King Chulalongkorn Memorial Hospital.

I would like to thank medical staff at the Vascular and Interventional Radiology Unit, Department of Radiology, King Chulalongkorn Memorial Hospital for their kindness in allowing for the research instrument and providing suggestions for improvement.

I am grateful to all the lecturers and staff of Medical Imaging, for supplying me academic knowledge in Medical Imaging.

Finally, I am grateful to my family for their financial support, entire care, and love. The usefulness of this thesis, I dedicate to my father, my mother and all the teachers.

ศูนย์วิทยทรัพยากร  
จุฬาลงกรณ์มหาวิทยาลัย

# CONTENTS

	<b>Page</b>
ABSTRACT (THAI).....	iv
ABSTRACT (ENGLISH).....	v
ACKNOWLEDGEMENTS.....	vi
CONTENTS.....	vii
LIST OF TABLES.....	x
LIST OF FIGURES.....	xi
LIST OF ABBREVIATIONS.....	xiii
<b>CHAPTER I INTRODUCTION</b>	
1.1 Background and rationale.....	1
1.2 Objectives.....	1
<b>CHAPTER II REVIEW OF RELATED LITERATURE</b>	
2.1 Introduction.....	2
2.1.1 Fluoroscopic equipment.....	2
2.1.2 Thermoluminescent dosimetry.....	4
2.1.3 Dose area product (DAP) meter .....	11
2.1.4 Dosmetric quantities.....	12
2.1.5 Dosmetric quantities related to stochastic and deterministic effects.....	12
2.1.6 Uncertainty in measurement.....	14
2.2 Review of related literatures.....	16
<b>CHAPTER III RESEARCH METHODOLOGY</b>	
3.1 Research design.....	18
3.2 Research design model.....	18
3.3 Conceptual framework.....	19

	<b>Page</b>
3.4 Research questions.....	19
3.4.1 Primary research questions.....	19
3.4.2 Secondary research questions.....	19
3.5 Keywords.....	19
3.6 The sample.....	20
3.6.1 Target population.....	20
3.6.2 Sample population.....	20
3.6.3 Eligible criteria.....	20
3.6.4 Sample size determination.....	20
3.7 Materials.....	21
3.7.1 Radiographic-fluoroscopic system.....	21
3.7.2 Unfors model Xi.....	21
3.7.3 Thermoluminescent dosimeter (TLD).....	22
3.7.4 Automatic TLD reader.....	22
3.7.5 DAP meter.....	23
3.7.6 Portal film.....	23
3.7.7 The patients.....	23
3.8 Methods.....	24
3.9 Measurement.....	24
3.10 Data collection.....	24
3.11 Data analysis.....	25
3.12 Expected benefit.....	25
3.13 Ethical consideration.....	25



**CHAPTER IV RESULTS**

4.1 The quality control of Radiographic-Fluoroscopic System.....	26
4.2 The data of patient studies.....	26
4.3 Thermoluminescent dosimeter calibration.....	28
4.3.1 Sensitivity of TLD-100 chips.....	28
4.3.2 Linearity of TLD-100 chips.....	28
4.3.3 Minimum detectable dose.....	29
4.4 Measurement of radiation dose in medical staff.....	30
4.4.1 Patients at prone position.....	30
4.4.2 Patients at left lateral position.....	31
4.5 Measurement of dose area product in patient.....	33
4.6 The relationship between the patient dose and medical staff dose.	35

**CHAPTER V DISCUSSION AND CONCLUSION**

5.1 Discussion.....	38
5.2 Conclusion.....	40
5.3 Recommendations.....	40

<b>REFERENCES</b> .....	41
-------------------------	----

<b>APPENDICES</b> .....	43
-------------------------	----

Appendix A: Patient information sheet and consent form.....	44
Appendix B: Information sheet.....	51
Appendix C: Case record form.....	54
Appendix D: Report the radiation dose profile survey.....	55

<b>VITAE</b> .....	58
--------------------	----

## LIST OF TABLES

<b>Table</b>	<b>Page</b>
2.1 Radiation weighting factor.....	13
2.2 $W_T$ -new recommendations from Impact of the new ICRP recommendations on external radiation protection dosimetry.....	14
4.1 Patient data at prone position.....	26
4.2 Patient data at left latera position.....	27
4.3 Reading values of background.....	29
4.4 The radiation dose to the first medical staff at patient prone position, measured by TLD-100.....	30
4.5 The radiation dose to the second medical staff at patient prone position, measured by TLD-100.....	30
4.6 The radiation dose to the first medical staff at patient left lateral position, measured by TLD-100.....	31
4.7 The radiation dose to the second medical staff at patient left lateral position, measured by TLD-100.....	31
4.8 The ratio of averaged values between occupational doses and dose-area product in $\mu\text{Gy}/10\text{Gy}\cdot\text{cm}^2$ from TLD reading at five locations on medical staff and from DAP.....	37
5.1 DAP values from this study and DRL (UK).....	38
5.2 Average DAP for therapeutic ERCP.....	39
5.3 Calculation of the first medical staff dose per year at different organs from ERCP procedure.....	39
5.4 Calculation of the second medical staff dose per year at different organs from ERCP procedure.....	40

## LIST OF FIGURES

<b>Figure</b>	<b>Page</b>
2.1 Block diagram of the thermoluminescence dose measurement.....	4
2.2 A simplified energy-level diagram of thermoluminescence process.....	5
2.3 The glow curve of lithium fluoride (TLD-100).....	6
2.4 An example of thermoluminescence versus absorbed dose curve for TLD-100 powder.....	7
2.5 Relation of half value layer to effective energy.....	8
2.6 Theoretical sensitivity of thermoluminescence phosphors.....	9
3.1 The research design model.....	18
3.2 Conceptual framework.....	19
3.3 Radiographic-Fluoroscopic system, Siemens Medical Solutions, Model Polystar.....	21
3.4 Unfors Model Xi for QC of X-ray machine.....	19
3.5 Thermoluminescent dosimeter (TLD).....	22
3.6 The Harshaw Model 5500 automatic thermoluminescent dosimeter reader	22
3.7 Dose Area Product meter (DAP) Model PTW-Diamentor E.....	23
3.8 Film Kodak X – O Mat V.....	23
3.9 Place TLDs on different sites on gastroenterologist.....	24
4.1 Linearity of LiF TLD-100 when irradiated at various doses for 80 kVp....	28
4.2 Linearity of LiF TLD-100 when irradiated at various doses for 100 kVp...	29
4.3 The average dose ( $\mu\text{Gy}$ ) to the first and second medical staff at patient prone position.....	32
4.4 The average dose ( $\mu\text{Gy}$ ) to the first and second medical staff at patient left lateral position.....	32

## LIST OF FIGURES (continued)

<b>Figure</b>	<b>Page</b>
4.5 The average dose ( $\mu\text{Gy}$ ) to the first medical staff at two positions.....	32
4.6 The average dose ( $\mu\text{Gy}$ ) to the second medical staff at two positions.....	32
4.7 The relation between patient dose ( $\text{cGy}\cdot\text{cm}^2$ ) at prone position and dose to left forearm of the first medical staff ( $\mu\text{Gy}$ ).....	33
4.8 The relation between patient dose ( $\text{cGy}\cdot\text{cm}^2$ ) at prone position and dose to left forearm of the second medical staff ( $\mu\text{Gy}$ ).....	33
4.9 The relation between patient dose ( $\text{cGy}\cdot\text{cm}^2$ ) at left lateral position and dose to left forearm of the first medical staff ( $\mu\text{Gy}$ ).....	34
4.10 The relation between patient dose ( $\text{cGy}\cdot\text{cm}^2$ ) at left lateral position and dose to left forearm of the second medical staff ( $\mu\text{Gy}$ ).....	34

  
 ศูนย์วิทยทรัพยากร  
 จุฬาลงกรณ์มหาวิทยาลัย

## LIST OF ABBREVIATIONS

<b>Abbreviation</b>	<b>Terms</b>
AAPM	American Association of Physicists in Medicine
Al <sub>2</sub> O <sub>3</sub>	Aluminum Oxide
B	The back scatter factor
BG	The background
CaCO <sub>3</sub>	Calcium carbonate
CaF <sub>2</sub>	Calcium fluoride
CaSO <sub>4</sub>	Calcium sulphate
cGy	Centigray
cGy cm <sup>2</sup>	Centigray centimeter square
<sup>60</sup> Co	Cobalt-60
<sup>137</sup> Cs	Cesium-137
CsI	Cesium iodide
°C	Degree Celsius
DAP	The dose-area product
ECC	The element correction coefficient
ED	The effective dose
ERCP	Endoscopic retrograde cholangiopancreatography
ESD	Entrance Skin Dose
Gy	Gray
Gy cm <sup>2</sup>	Gray centimeter square
HVL	Half-Value Layer
IAEA	International Atomic Energy Agency



## LIST OF ABBREVIATIONS (continued)

<b>Abbreviation</b>	<b>Terms</b>
ICRU	International Commission on Radiation Units and Measurements
II	Image intensifier
kVp	Kilo voltage peak
keV	Kiloelectron voltage
Li <sub>2</sub> B <sub>4</sub> O <sub>7</sub>	Lithium borate
LiF	Lithium fluoride
m	Meter
mA	Milliampere
mAs	Milliampere second
MDD	Minimum detectable dose
MeV	Megaelectron voltage
mGy	Milligray
mm	Millimeter
mm Al	Millimeter aluminum
mrad	Millirad
n	Neutron
nC	Nanocoulomb
PC	Personal computer
PMT	Photomultiplier tube
QA	Quality Assurance
QC	Quality Control
Q <sub>ci</sub>	The correction charge integral

**LIST OF ABBREVIATIONS (continued)**

<b>Abbreviation</b>	<b>Terms</b>
$Q_i$	The charge integral value
r	The correlation coefficient
RCF	The reader calibration factor
RPO	The right posterior oblique
SD	Standard Deviation
SID	Source to Image Distance
TLD	Thermoluminescent Dosimeter
TTP	Time temperature profile
UK	United Kingdom
VC	The variation coefficient
Z	Atomic number
$\mu\text{Gy}$	Microgray

ศูนย์วิทยทรัพยากร  
จุฬาลงกรณ์มหาวิทยาลัย

# CHAPTER I

## INTRODUCTION

### 1.1 Background and rationale

Fluoroscopy is a type of x-ray real time image which allows radiologist to view an area of interest as an x-ray beam pass through the body part being examined and transmitted to a monitor. An intravenous injection of contrast material is used to highlight the area, making it a very bright, white image on monitor. The fluoroscopy is an imaging technique commonly used to obtain the internal structures of a patient. Fluoroscopic system consists of an x-ray source and fluorescent screen. However, modern fluoroscopes couple the screen to an x-ray image intensifier (II) and charge-coupled device (CCD) video camera allowing the images to be recorded and played on a monitor. Fluoroscopic procedures may produce high radiation doses to patient depend on the type of procedure which endoscopic retrograde cholangiopancreatography (ERCP) is one procedure in fluoroscopic study.

ERCP has been established for over 35 years. ERCP is a non-invasive technique that combines the use of endoscopy and fluoroscopy to diagnose and treat certain problems of the biliary or pancreatic ductal systems. It is an x-ray examination of the bile ducts which is aided by a video endoscope. ERCP is usually performed with the patient in the prone or left lateral position. The supine position could be more comfortable and may facilitate airway management. ERCP is also used to diagnose and treat gallstones, inflammatory strictures leaks and cancer. The use of x-rays and endoscopy has been combined, which a long, flexible, lighted tube has been used. Advanced Endoscopic procedure utilizes fluoroscopy to obtain cholangiograms and/or pancreatograms. As the procedure takes about 20 – 60 minutes, it may cause the radiation risk to patients and medical staff.

Previous study at our department concerned the radiation dose to patients and medical staff during ERCP. The procedures currently perform in prone position and sometimes the left lateral position. As our knowledge, there is no available report on the radiation dose to the patients and medical staff during ERCP from the left lateral position. Therefore, the determination of radiation doses to the patients and medical staff during ERCP at both prone and left lateral positions should be performed.

### 1.2 Objectives

1.2.1 To evaluate the radiation dose to patient at two positions (prone and left lateral) and medical staff during ERCP procedure using DAP meter and TLD.

1.2.2 To relate the patient dose and medical staff dose for two patient positions, during ERCP procedure.

## CHAPTER II

### REVIEW OF RELATED LITERATURES

#### 2.1 Introduction

##### 2.1.1 Fluoroscopic Equipment

The simple type of fluoroscopic system consists of an under couch x-ray tube and an over couch image intensifier system. The type of imaging equipment of portable C-arm with a vascular package software is either floor or ceiling mounted C-arms. The fixed units generally allow higher definition imaging and more facile movement of devices by allowing the operator to control both the imaging unit and bed position. However, regardless of the specific imaging system, the essentials of fluoroscopy are unchanged and can be achieved with each system.

##### 2.1.1.1 Basic Principles of Fluoroscopy

Roentgen discovery of x-rays related directly to fluoroscopy, because fluorescence on the material in the room caused him to take note of the x-ray properties. In 1896, Thomas A. Edison created the fluoroscope, consisting of a zinc-cadmium sulfide screen that was placed above the patient's body in the x-ray beam. In first-generation units, the radiologist stared directly at a faint yellow-green fluorescent image through a sheet of lead to prevent the x-ray beam from striking his or her eyes. The exam room required complete darkness and the radiologist had to first wear red goggles for up to 20 or 30 minutes to adapt the eyes to darkness to see a faint fluorescent image.

The dynamic design of fluoroscopy enables real-time radiographic imaging of moving anatomic structures. Generally, fluoroscopy procedures require a radiologist to perform and monitor the examination, and to view the live study. A continuous beam from an x-ray tube placed beneath the table passes through the patient and falls onto a fluorescent screen. The x-ray beam from the tube beneath the table passes through the patient to the film located above the patient. The x-ray tube can locate over table so that it can be used for conventional radiography as well.

Early generation fluoroscopic images presented particularly difficult viewing challenges for radiologists. The human retina contains 2 types of image receptors. Cones are operating more effectively in bright light, while rods are more sensitive to low light. Because rods are also more sensitive to blue-green light, the radiologists' red goggles filtered out blue-green wavelengths to allow the rods to recover peak sensitivity before viewing fluoroscopic images.

The dimness of the early images and required use of rod vision resulted in poor visual acuity and poor contrast distinction because rod vision does not lend itself to distinguish between shades of gray. To allow radiologists to use cone vision but minimize patient exposure, the industry developed the image-intensifier tube. The image intensifier amplifies the faint light pattern emitted by the fluorescing screen and the radiologist views the image on a monitor. Fluoroscopic imaging is very useful in evaluating dynamic anatomic structures, such as gastrointestinal functions, diaphragmatic movement of respiration and cardiac functions. Fluoroscopy is also valuable in performing studies that require continuous imaging and monitoring.

### 2.1.1.2 Fluoroscopy Systems

While the x-ray tube rests under the patient table, the fluoroscopic image intensifier is located above the table. Typical fluoroscopic x-ray tube currents are 1 to 5 mA, compared to 50 to 500 mA for conventional radiographic tubes. The table supporting the patient usually rotates to an upright position for certain examinations and can be lowered to horizontal position for other procedures. These technologies are available to record images created during fluoroscopic procedures.

### 2.1.1.3 Image Intensifier

The image intensifier plays a key role in increasing image brightness without forcing increased radiation exposure by converting the transmitted x-rays into a brightened, visible light image. The intensifier input phosphor converts x-ray photons to light photons, which then are converted to photoelectrons within a photocathode. A series of electrodes strikes the output phosphor, accelerating and focusing the electrons into light photons that can be captured by a number of different imaging devices.

Early generation of image intensifier had small input size and a glass vacuum case. The later models come with large input field sizes up to 57 cm in diameter with little image distortion. The tubes now are encased in metal to protect the glass vacuum envelope. The outer most component of the intensifier is the input window, which is convex and made to minimize x-ray absorption, scatter and cost. Just behind the window lies the layer of input phosphor, cesium iodide (CsI), which converts the x-ray energy into visible light. The CsI crystals are grown as tiny, tightly packed needles that offer excellent spatial resolution and little dispersion. Input layer thickness is a compromise of spatial resolution versus x-ray absorption efficiency. The thicker phosphor layers offer higher x-ray absorption efficiency.

Bound to the input phosphor is the photocathode, the layer made up of antimony-cesium. These compounds emit electrons when stimulated by light, a process called photoemission. To maximize efficiency of conversion from light photon to photoelectron, the light emitted from the input phosphor should match the photocathode sensitivity spectrum. The photocathode accelerates photoelectrons to the anode at the back of the intensifier. Those are focused down to the size of the output phosphor by a series of electrostatic focusing electrodes that are very sensitive to external electrical and magnetic fields. Therefore, possible external influences of nearby magnetic resonance imaging units or unstable high voltages must be monitored to prevent distortion of fluoroscopic image quality.

When the high-energy electrons reach and interact with the output phosphor, they produce a considerable amount of light. Typically, the output phosphor consists of a compound made of silver-activated zinc-cadmium sulfide (ZnCdS:Ag). The ratio of the number of light photons at the output phosphor to the number of x-rays at the input phosphor is called the flux gain and is the reason for the increased illumination. Image monitoring can help control brightness and depends primarily on the anatomic structure under study. As with other imaging techniques, operators can control kVp and mA, and these factors affect both image quality and patient exposure. Generally, high kVp and low mA are preferred for fluoroscopy.



### 2.1.2 Thermoluminescent dosimetry (TLD) [1]

A radiation dosimeter is a device, instrument or system that measures or evaluates, either directly or indirectly, the quantities exposure, kerma, absorbed dose or equivalent dose, or their time derivatives (rates), or related quantities of ionizing radiation. A dosimeter along with its reader is referred to as a dosimetry system.

Measurement of a dosimetric quantity is the process of finding the value of the quantity experimentally using dosimetry systems. The result of a measurement is the value of a dosimetric quantity expressed as the product of a numerical value and an appropriate unit.

In recent years many applications of thermoluminescent dosimeter have been reported in the literature. The small size, good energy dependence, good sensitivity and large useful dose range of thermoluminescent dosimeter are key advantages, as the direct measurement of dose is possible under conditions in which other forms of dosimetry are not practical; measurement of the dose from the primary beam during fluoroscopy is convenient since the dosimeter does not interfere with the study.[2]

There are several solid state systems available for the dosimetry of ionizing radiation. However, none of the system provide absolute measurement-each needs calibration in a known radiation field before it can be used for the determination of absorbed dose. There are two types of solid dosimeters: (a) integrating type dosimeters (thermoluminescent crystal, radiophotoluminescent glasses, optical density type dosimeters such as glass and film), and (b) electrical conductivity dosimeters (semiconductor junction detectors, induced conductivity in insulating materials). Of these, the most widely used systems for the measurement of absorbed dose are the thermoluminescent dosimeter, diode and film.

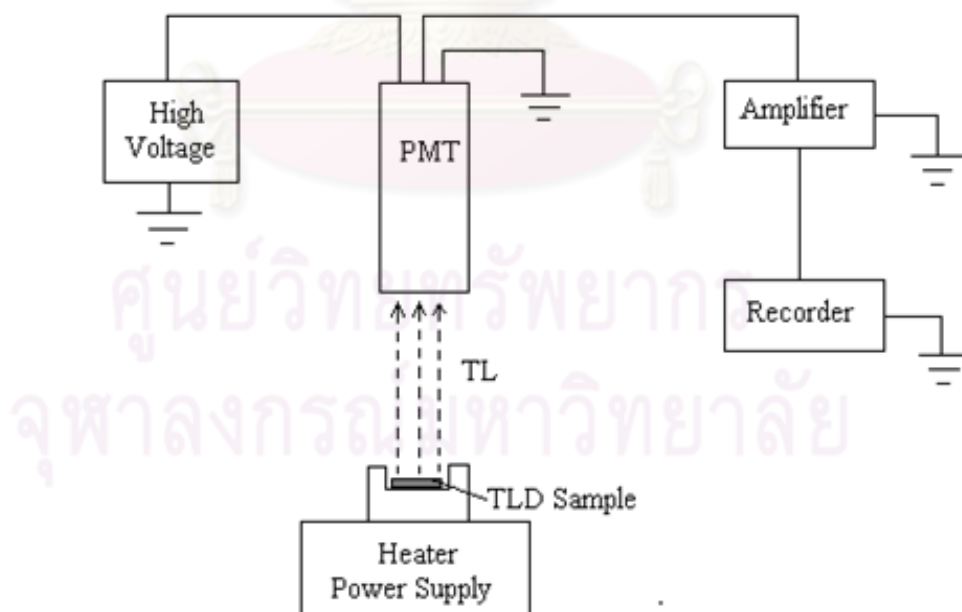


**Figure 2.1** Block diagram of the thermoluminescence dose measurement.

Many crystalline materials exhibit the phenomenon of thermoluminescence used in thermoluminescent dosimeter. When, such as a crystal is irradiated, a very minute fraction of the absorbed energy is stored in the crystal lattice. Some of this energy can be recovered later as visible light if the material is heated. This phenomenon of release of visible photons by thermal mean is known as thermoluminescence.

The arrangement for measuring the thermoluminescence output is shown in figure 2.1. The radiation material is placed in a heater cup or planchet, where it is heated for a reproducible heating cycle. The emitted light is measured by photomultiplier tube (PMT) which converts light into an electrical current. The current is then amplified and measured by a recorder or a counter.

There are several thermoluminescent phosphors available such as lithium fluoride (LiF), lithium borate ( $\text{Li}_2\text{B}_4\text{O}_7$ ), and calcium fluoride ( $\text{CaF}_2$ ). Of these phosphors, LiF is most extensively studied and most frequently used thermoluminescence for the photons. But the presence of a trace amount of impurities (e.g., magnesium) provides the radiation-induced thermoluminescence. These impurities give rise to imperfections in the lattice structure of LiF and appear to be necessary for the appearance of the thermoluminescence phenomenon.

#### 2.1.2.1 Thermoluminescent dosimeter

The chemical and physical theory of thermoluminescent dosimeter is not exactly known, but simple models have been proposed to explain the phenomenon qualitatively. Figure 2.2 shows an energy-level diagram of an inorganic crystal exhibiting thermoluminescence by ionizing radiation.

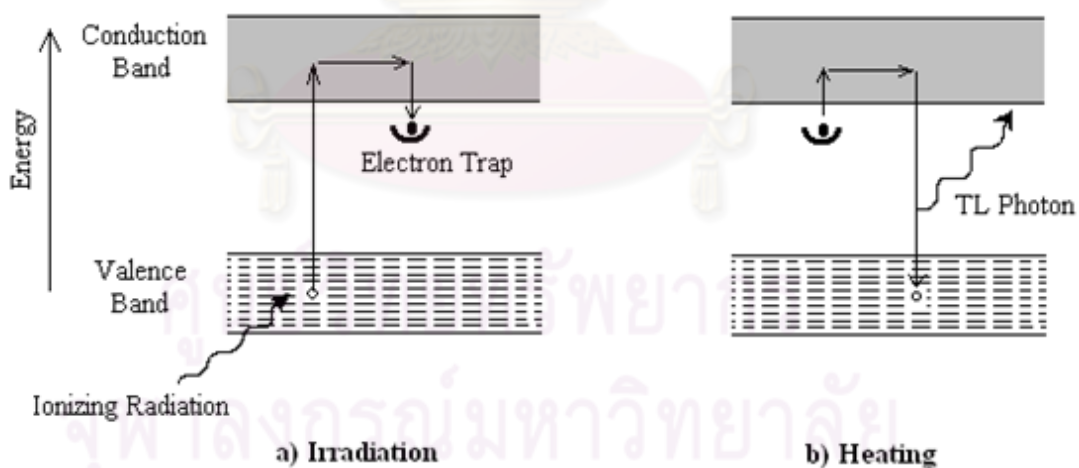


**Figure 2.2** A simplified energy-level diagram of thermoluminescence process.

In an individual atom, electron occupies discrete energy levels. In a crystal lattice, on the other hand, electronic energy levels are perturbed by mutual interactions between atoms and give rise to energy bands the “allow” energy bands and the forbidden energy bands. In addition, the presence of impurities in the crystal creates energy trap in the forbidden region, providing metastable states for the electrons. When the material is irradiated, some of the electrons in the valence band

(ground state) receive sufficient energy to be raised to the conduction band. The vacancy thus created in the valence band is called a positive hole. The electron and the hole move independently through their respective bands until they recombine or until they fall into a trap (metastable state).

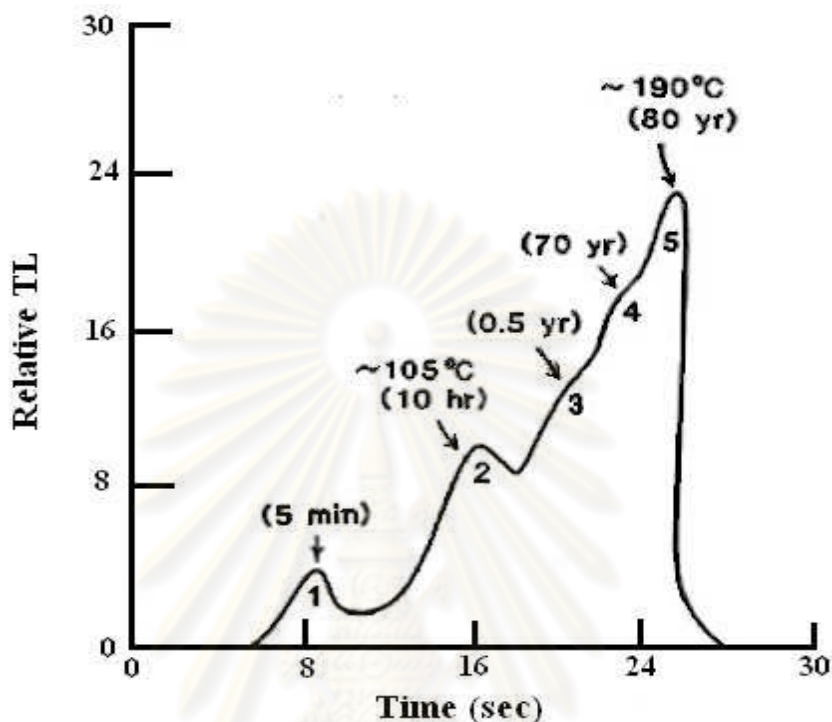


**Figure 2.3** The glow curve of lithium fluoride (TLD-100).

A plot of thermoluminescence against temperature is called a *glow curve* (Figure 2.3.). As the temperature of the thermoluminescence material exposed to radiation is increased, the probability of releasing trapped electrons increases. The light emitted first increases, reach a maximum value, and fall again to zero. Because most phosphors contain a number of traps at various energy levels in the forbidden band, the glow curve may consist of a number of glow peaks as shown in figure 2.3. The different peaks correspond to different ‘trapped’ energy levels.

#### 2.1.2.2 Lithium fluoride

Lithium fluoride has an effective atomic number of 8.2 compared with 7.4 for soft-tissue. This makes this material very suitable for clinical dosimetry. The dose absorbed in LiF can be converted to dose in muscle by considerations similar to those discussed earlier. For example, under electronic equilibrium conditions, the ratio of absorbed dose in the two media will be the same as the ratio of their mass energy absorption coefficient. If the dimensions of the dosimeter are smaller than the ranges of the electron crossing the dosimeter, then the Bragg-Gray relationship can also be used. The ratio of absorbed doses in the two media will be the same as the ratio of mass stopping power. The applicability of the Bragg-gray cavity theory to thermoluminescent dosimeter has been discussed by several authors.

### 2.1.2.3 Practical considerations

The thermoluminescent dosimeter must be calibrated before use. The response of the thermoluminescent dosimeter materials is affected by radiation history and thermal history, the material must be suitably annealed to remove residual effect. The standard pre-irradiation annealing procedure for LiF is 1 hour of heating at 400 °C and then 24 hour at 80 °C. The slow heating, namely 24 hour at 80 °C, remove peak 1 and 2 of the glow curve by decreasing the ‘trapping efficiency’. Peak 1 and 2 can also be eliminated by post-irradiation annealing for 10 minute at 100 °C. The need for eliminating peak 1 and 2 arise from the fact that the magnitude of these peaks decreases relatively fast with time after irradiation. By removing these peaks by annealing, the glow curve becomes more stable and therefore predictable

The dose response curve for TLD-100 is shown in figure 2.4. The curve is generally linear up to  $10^3$  cGy but beyond this it becomes supralinear. The response curve, however, depends on many conditions that have to be standardized to achieve reasonable accuracy with thermoluminescent dosimeter. The calibration should be done with the same thermoluminescent dosimeter reader, in approximately the same quality beam and to approximately the same absorbed dose level.

The thermoluminescent dosimeter response is defined as thermoluminescence output per unit absorbed dose in the phosphor. Figure 2.6 gives the energy response curve for LiF (TLD-100) for photon energies below megavoltage range. The studies of energy response for photons above  $^{60}\text{Co}$  and high energy electrons have yield somewhat conflicting results.

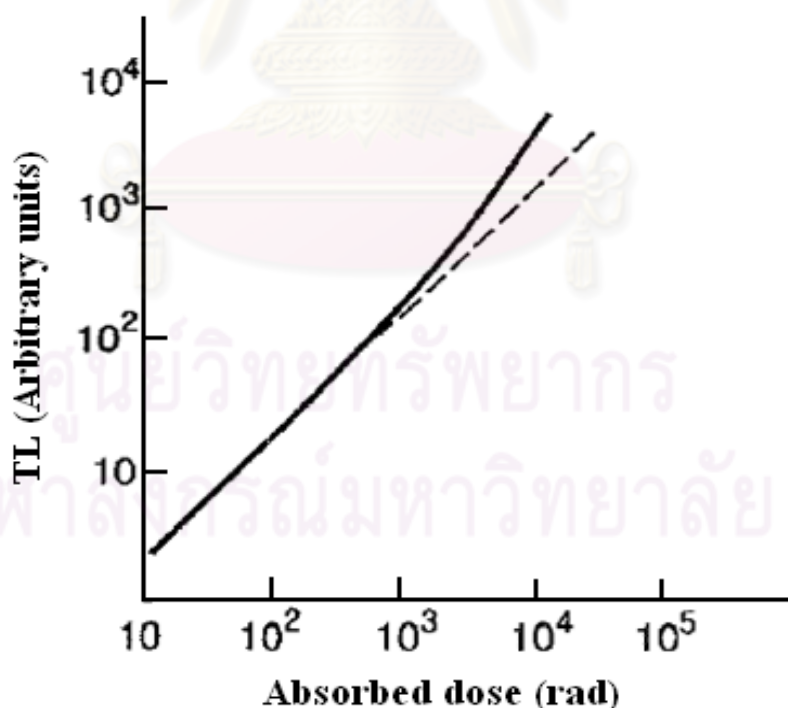


**Figure 2.4** An example of thermoluminescence versus absorbed dose curve for TLD-100 powder.

When considerable care is used, precision of approximately 3% may be obtained using thermoluminescent dosimeter powder or extruded material. Although not as precise as the ion chamber, thermoluminescent dosimeter's main advantage is in measuring dose in regions where ion chamber cannot be used. For example, thermoluminescent dosimeter is extremely useful for patient dosimetry by direct insertion into tissue or body cavities. Since thermoluminescent dosimeter material is available in many forms and sizes, it can be used for special dosimetry situation such as for measuring dose distribution in the build-up region, around brachytherapy source, and for personal dose monitoring.

#### 2.1.2.4 Energy response

The photoelectric absorption process is usually the predominant absorption process at low ( $< 100$  keV) photon energies. This interaction, which involves the innermost electrons, is dependent on the nuclear charge of the atom, the atomic number ( $Z$ ). Consequently, radiation detectors with high atomic number show a greatly enhanced response at the low photon energies. The energy response of a detector at the particular photon energy may be defined as the response of the detector at that photon energy relative to its response at some reference energy (usually 1-3 MeV) where the photoelectric absorption process is largely inoperative. The dosimeter is said to have a good energy response if its response per roentgen shows little change with photon energy, the energy response is poor if this change is large. Detectors with an effective atomic number approximately that of air ( $Z = 7.64$ ) show a good energy response while those with an effective atomic number much different from 7.64 show a poor energy response.

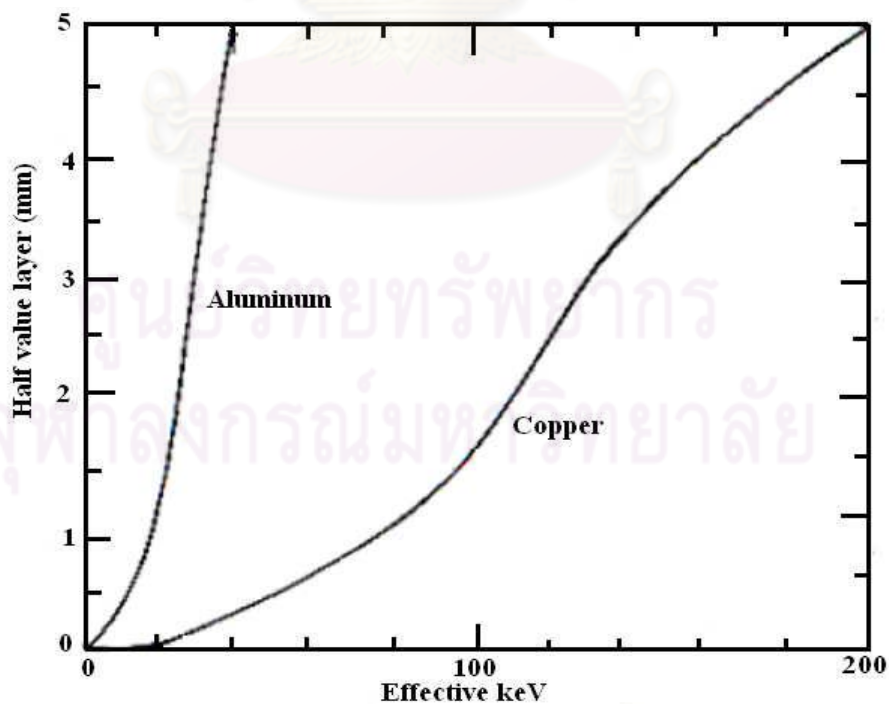


**Figure 2.5** Relation of half value layer to effective energy.



One recurring problem in dealing with energy response is the precise statement of x-ray beam quality. If the radiation source is a monoenergetic gamma-ray emitter (for example,  $^{137}\text{Cs}$ ) then the beam quality can be expressed simply and accurately as the monoenergetic photon energy (662 keV). On the other hand, if the radiation source used is an x-ray generator that produces a spectrum of photon energies up to the maximum accelerating voltage, then specification of the beam quality is much more difficult. Beam quality may be expressed in terms of 'effective keV' defined as that monoenergetic photon energy which has the same half value layer as dose the x-ray beam in question. Conversion from the measured half value layer or effective energy (keV) can be made from figure 2.5. Effective energy (keV) determine in this manner is not a highly precise statement of quality for example, two x-ray beams generated at different accelerating voltages and with different filtrations can have identical half value layer (and consequently the same effective energy). It is often valuable to specify the first and second half value layer as well as the accelerating voltage and the amount of filtration.

There are two ways to determine energy response curves for thermoluminescent phosphors by using experimentally determined value based on calculated value from available absorption coefficients for the various photon energies. Experimentally measured values are usually more appropriate when correcting for the energy response in various experimental irradiations. Figure 2.6 shows energy responses curve which were calculated by comparing the absorption coefficient of the various thermoluminescent phosphors with the energy deposited in tissue. Energy response is usually related to the exposure in air rather than to the dose in tissue. ((1)  $\text{CaSO}_4$ ; (2)  $\text{CaF}_2$ ; (3)  $\text{Al}_2\text{O}_3$ ; (4)  $\text{LiF}$ ; (5)  $\text{CaCO}_3$ ; (6)  $\text{SiO}_2$ ; and (7)  $\text{Li}_2\text{B}_4\text{O}_7$ )

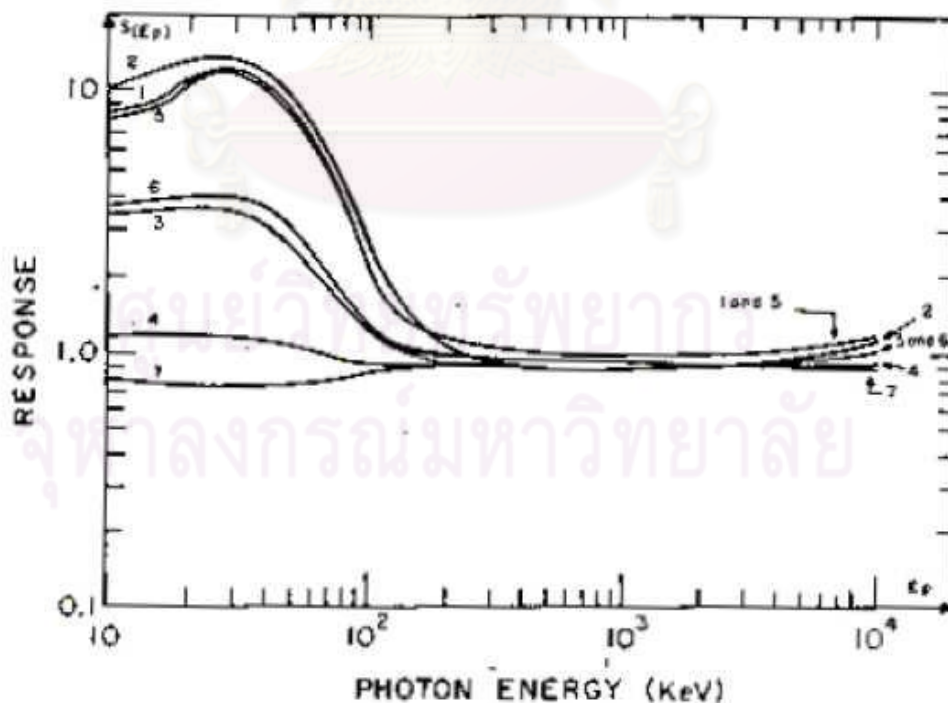


**Figure 2.6** Theoretical sensitivity of thermoluminescence phosphors.

### 2.1.2.5 Calibration of thermoluminescent dosimeter [3]

The purpose of calibrating a thermoluminescent dosimeter instrument is to produce consistent and accurate reading in dosimetrically meaningful units. The calibration process involves the following 3 steps.

#### A) Generate calibration dosimeter

In this process, an element correction coefficient (ECC) is generated by using a set of dosimeters, typically 1-2% of the total population to be calibration dosimeters. They are identified and segregated from the field dosimeters.

All dosimeters are annealed to clear them all residual exposure. Duration time between annealing and exposing should be the same for all dosimeters. After being exposed to the known radiation dose, the charge integral value ( $Q_i$ ) in nanocoulomb (nC) of each dosimeter ( $i$ ) is read out and recorded. Then the average charge integral ( $\bar{Q}$ ) of all dosimeters is calculated and the element correction coefficient ( $ECC_i$ ) for individual dosimeter  $i$  ( $i = 1, 2, 3, \dots, n$ ) is computed by dividing the average charge integral by the individual charge ( $Q_i$ ) as:

$$ECC_i = \frac{\bar{Q}}{Q_i} \quad (2.1)$$

#### B) Calibration of thermoluminescent dosimeter reader

A group of dosimeters about 1 – 2 % of dosimeters in (a) which have  $ECC_i$  value close to 1 are chosen to be calibration dosimeters. The calibration dosimeters are exposed to known amount of radiation dose ( $D$ ) in grays and read by TLD reader. As ( $Q_i$ ) is the reading for the dosimeter  $i$ , the corrected charge integral ( $Q_{ci}$ ) of the dosimeter is calculated by:

$$Q_{ci} = Q_i \times ECC_i \quad (2.2)$$

Then the reader calibration factor (RCF) is calculated from the equation:

$$RCF = \frac{\bar{Q}_c}{D} \quad (2.3)$$

When  $\bar{Q}_c$  is the average corrected charge integral and calculated by:

$$\bar{Q}_c = \frac{1}{n} (\sum_{i=1}^n Q_{ci}) \quad (2.4)$$

#### C) Calibration of dosimeter

The rest of the dosimeter [number of the dosimeters in (a) – number of dosimeters in (b)] is used as field dosimeters. They are exposed by the known radiation dose of  $L$  grays and read by TLD reader. The calibration value of element correction coefficient for individual dosimeter ( $ECC_{ci}$ ) is then calculated by:

$$ECC_{ci} = \frac{(RCF \times L)}{Q_i} \quad (2.5)$$

#### 2.1.2.6 Determination of unknown radiation dose

The field dosimeters in 2.1.2.5 (C) are used to measure unknown radiation dose. The unknown dose  $D$  in grays is calculated by using  $ECC_{ci}$  from the equation:

$$D = \frac{(Q_i \times ECC_{ci})}{RCF} \quad (2.6)$$

When  $Q_i$  is the reading of the individual field dosimeter  $i$  of any user defined length.

#### 2.1.3 Dose area product (DAP)

Dose-area product is relatively easy to measure. DAP meters have been around for many years, and were actually used in the 1964 and 1970 U.S. X-ray Exposure Studies. Advocates of DAP meters contend that the DAP is a better indicator of risk than entrance dose alone, since DAP incorporates the entrance dose and field size. DAP has been shown to correlate well with the total energy imparted to the patient, which is related to the effective dose and therefore to overall cancer risk.

Dose-Area-Product (DAP) meters are large-area, transmission ionization chambers and associated electronics. In use, the ionization chamber is placed perpendicular to the beam central axis and in a location to completely intercept the entire area of the x-ray beam. The DAP, in combination with information on x-ray field size can be used to determine the average dose produced by the x-ray beam at any distance downstream in the x-ray beam from the location of the ionization chamber. A recent modification of the ionization chamber design used in a DAP meter has resulted in an instrument that measures both DAP and the dose delivered by the x-ray beam. This design effectively combines data from a small ionization chamber that is completely irradiated by the beam and independent of the collimator adjustments with the conventional DAP meter.

The dose-area product (DAP) meters are mostly installed in fluoroscopic and radiographic systems. DAP meters are used to measure the radiation dose to air (cGy), times the area of the X-ray field (cm<sup>2</sup>), on exposed area. The relationship between DAP and exposure-area product (EAP) is essentially a single conversion factor that relates dose to exposure. EAP is expressed in gray-cm<sup>2</sup> (Gy.cm<sup>2</sup>, usually read in cGy.cm<sup>2</sup>).

An ionization chamber larger than the area of the x-ray beam is placed just beyond the x-ray collimators. The DAP ionization chamber must intercept the entire x-ray field for an accurate reading, one proportional to the EAP. The reading from a DAP meter can be changed by altering the x-ray technique factors (kVp, mA, or time), varying the area of the field, or both. If the chamber area is larger than that of the collimators, as the collimators are opened or closed the charge collected will also increase or decrease in proportion to the area of the field. For example, a 5 x 5 cm<sup>2</sup> x-ray field with an entrance dose of 1 mGy will yield a 25 mGy.cm<sup>2</sup> DAP value. If the field is increased to 10 x 10 cm<sup>2</sup>, with the same entrance dose of 1 mGy the DAP increases to 100 mGy.cm<sup>2</sup>, which is 4 times the DAP for the 5 x 5 cm<sup>2</sup> field.

## 2.1.4 Dosmetric quantities [4]

### 2.1.4.1 The incident air kerma

The incident air kerma,  $K_i$ , is the kerma to air from an incident X-ray beam measured on the central beam axis at the position of the patient surface. Only the radiation incident on the patient or phantom and not the backscattered radiation is included. Unit: J/kg. The name for the unit of kerma is gray (Gy).

### 2.1.4.2 Entrance surface dose (ESD)

The entrance surface dose is defined as the absorbed dose in air at the point of intersection of the x-ray beam axis with the entrance surface of the patients,  $K_e$ , including back-scattered radiation,  $B$ , and a well defined equation 2.7.

$$K_e = K_i B \quad (2.7)$$

### 2.1.4.3 Air kerma–area product (Dose area product)

The air kerma–area product,  $P_{KA}$ , is the integral of the air kerma over the area of the X-ray beam in a plane perpendicular to the beam axis thus:

$$P_{KA} = \int_A K(x, y) dx dy \quad (2.8)$$

Unit:  $J \cdot kg^{-1} \cdot m^2$ . If the special name gray is used, the unit of air kerma–area product is  $Gy \cdot m^2$ . The air kerma–area product (Dose area product) has the useful property that it is approximately invariant with distance from the X ray tube focus (when interactions in air and extrafocal radiation can be neglected), as long as the planes of measurement and calculation are not so close to the patient or phantom that there is a significant contribution from backscattered radiation.

## 2.1.5 Dosmetric quantities related to stochastic and deterministic effects

### 2.1.5.1 Organ and tissue dose

The mean absorbed dose in a specified tissue or organ is given the symbol  $D_T$  in ICRU 51 [5]. It is equal to the ratio of the energy imparted,  $\dot{\epsilon}_T$ , to the tissue or organ to the mass,  $m_T$ , of the tissue or organ, thus

$$D_T = \frac{\dot{\epsilon}_T}{m_T} \quad (2.9)$$

The mean absorbed dose in a specified tissue or organ is sometimes simply referred to as the organ dose.

### 2.1.5.2 Equivalent dose

The equivalent dose,  $H_T$ , to an organ or tissue,  $T$ , is defined in ICRP 60 and ICRU 51. For a single type of radiation,  $R$ , it is the product of a radiation weighting factor,  $W_R$ , for radiation  $R$  and the organ dose,  $D_T$ , thus:

$$H_T = W_R D_T \quad (2.10)$$

Unit: J/kg. The special name for the unit of equivalent dose is sievert (Sv). The radiation weighting factor,  $W_R$ , allows for differences in the relative biological effectiveness of the incident radiation in producing stochastic effects at low doses in tissue or organ, T. For X-ray energies used in diagnostic radiology,  $W_R$  is taken to be unity.

**Table 2.1** Radiation weighting factor

Radiation	Energy range	Radiation weighting factor ( $W_R$ )
Gamma	all	1
Beta	all	1
Neutrons	< 10 keV	5
	10 keV – 100 keV	10
	> 100keV – 2 MeV	20
	> 2 MeV – 20 MeV	10
	> 20 MeV	5
Proton	> 2 MeV	5
Alpha particles	all	20
Fission fragments	all	20
Heavy nuclei	all	20

### 2.1.5.3 Effective dose (ED)

The effective dose,  $E$ , is defined in ICRP 60 and ICRU 51. It is the sum over all the organs and tissues of the body of the product of the equivalent dose,  $H_T$ , to the organ or tissue and a tissue weighting factor,  $W_T$ , for that organ or tissue, thus:

$$ED = \sum_T W_T H_T \quad (2.11)$$

The tissue weighting factor,  $W_T$ , for organ or tissue T represents the relative contribution of that organ or tissue to the total detriment arising from stochastic effects for uniform irradiation of the whole body.

Unit: J/kg. The special name for the unit of effective dose is sievert (Sv). The sum over all the organs and tissues of the body of the tissue weighting factors,  $W_T$ , is unity.



**Table 2.2**  $W_T$  – new recommendations from Impact of the new ICRP recommendations on external radiation protection dosimetry. [6]

ORGAN	ICRP26	ICRP60	ICRP103
Gonads	0.25	0.20	0.08
Bone marrow (red)	0.12	0.12	0.12
Lung	0.12	0.12	0.12
Breast	0.15	0.05	0.12
Thyroid	0.03	0.05	0.04
Bone surfaces	0.03	0.01	0.01
Remainder	0.30	0.05	0.12
Colon	-	0.12	0.12
Stomach	-	0.12	0.12
Bladder	-	0.05	0.04
Liver	-	0.05	0.04
Oesophagus	-	0.05	0.04
Skin	-	0.01	0.01
Salivary glands	-	-	0.01
Brain	-	-	0.01

(Source: 2007 Recommendations of the International Commission on Radiological Protection (ICRP Publication No. 103), Centre for Radiation, Chemical and Environmental Hazards, Health Protection Agency (HPA))

#### 2.1.6 Uncertainty in measurement [4, 7]

The uncertainty is a parameter that describes the dispersion of the measured values of a quantity; it is evaluated by statistical methods (type A) or by other methods (type B), has no known sign and is usually assumed to be symmetrical.

The error of measurement is the difference between the measured value of a quantity and the true value of that quantity.

- An error has both a numerical value and a sign.
- Typically, the measurement errors are not known exactly, but they are estimated in the best possible way, and, where possible, compensating corrections are introduced.
- After application of all known corrections, the expectation value for errors should be zero and the only quantities of concern are the uncertainties.

A type A evaluation will normally be used to obtain a value for the repeatability or randomness of a measurement process. For some measurements, the random component of uncertainty may not be significant in relation to other contributions to uncertainty. It is nevertheless desirable for any measurement process that the relative importance of random effects be established. When there is a significant spread in a sample of measurement results, the arithmetic mean or average of the results should be calculated. If there are  $n$  independent repeated values for a quantity  $Q$  then the mean value  $\bar{q}$  is given by

$$\bar{q} = \frac{1}{n} (\sum_{j=1}^n q_j) = \frac{q_1 + q_2 + q_3 + \dots + q_n}{n} \quad (2.12)$$

The spread in the results gives an indication of the repeatability of the measurement process, which depends on various factors, including the apparatus used, the method, and sometimes on the person making the measurement. A good description of this spread of values is the standard deviation  $\sigma$  of the  $n$  values that comprise the sample, which is given by

$$\sigma = \sqrt{\frac{1}{n} \sum_{j=1}^n (q_j - \bar{q})^2} \quad (2.13)$$

This expression yields the standard deviation  $\sigma$  of the particular set of values sampled. However, these are not the only values that could have been sampled. If the process is repeated, another set of values, with different values of  $\bar{q}$  and  $\sigma$ , will be obtained.

For the large values of  $n$ , these mean values approach the central limit of a distribution of all possible values. This probability distribution can often be assumed to have the normal form.

As it is impractical to capture all values that are available, it is necessary to make an estimate of the value of  $\sigma$  that would be obtained were this possible. Similarly, the mean value obtained is less likely to be the same as that which would be obtained if a very large number of measurements could be taken, therefore an estimate has to be made of the possible error from the “true” mean.

From the equation 2.6 gives the standard deviation for the sample actually selected, rather than of the whole population of possible samples. However, from the results of a single sample of measurements, an estimate,  $s(q_j)$ , can be made of the standard deviation  $\sigma$  of the whole population of possible values of the measured from the relation.

$$s(q_j) = \sqrt{\frac{1}{n-1} \sum_{j=1}^n (q_j - \bar{q})^2} \quad (2.14)$$

The mean value  $\bar{q}$  will be derived from a finite number  $n$  of samples and therefore its value will not be the exact mean that would have been obtained if an infinite number of samples could have been taken. The mean value itself therefore has uncertainty. This uncertainty is referred to as the experimental standard deviation of the mean. It is obtained from the estimated standard deviation of the population by the expression.

$$s(\bar{q}) = \frac{s(q_j)}{\sqrt{n}} \quad (2.15)$$

The standard uncertainty is then the standard deviation of the mean. This is known as the *standard uncertainty* and is given the symbol  $u_i(x)$ .

$$u_i(x) = s(\bar{q}) \quad (2.16)$$

Once the standard uncertainties  $x_i$  and the sensitivity coefficients  $c_i$  have been evaluated, the uncertainties have to be combined in order to give a single value of

uncertainty to be associated with the estimate  $y$  of the measurement  $Y$ . This is known as the *combined standard uncertainty* and is given the symbol  $u_c(y)$ .

The combined standard uncertainty is calculated as follow:

$$u_c(y) = \sqrt{\sum_{i=1}^N c_i^2 u^2(x_i)} = \sqrt{\sum_{i=1}^N u_i^2(y)} \quad (2.17)$$

The GUM recognizes the need for providing a high level of confidence - referred to herein as *coverage probability* – associated with an uncertainty and uses the term *expanded uncertainty*,  $U$ , which is obtained by multiplying the combined standard uncertainty by a coverage factor. The coverage factor is given the symbol  $k$ , thus the expanded uncertainty is given by

$$U = k u_c(y) \quad (2.18)$$

In accordance with generally accepted international practice, it is recommended that a coverage factor of  $k = 2$  is use to calculate the expanded uncertainty. This value of  $k$  will give a coverage probability of approximately 95%, assuming a normal distribution.

Note: A coverage factor of  $k = 2$  actually provides a coverage probability of 95.45% for a normal distribution. For convenience this is approximated to 95% which would relate to a coverage factor of  $k = 1.96$ . However, the difference is not generally significant since, in practice, the coverage probability is usually based on conservative assumptions and approximations to the true probability distributions.

## 2.2 Review of related literature

Larkin CJ et al. [8] studied the radiation doses to patients during ERCP. Dose area product (DAP) measurements was used to estimate an effective dose (ED) to patients undergoing ERCP. This measure allows radiation risk associated with such procedures to be quantified. The aim of this study was to evaluate the ED to patients undergoing ERCP. Average effective dose from 20 subjects and the mean ED were estimated by using DAP readings and Monte Carlo computer software to model radiation exposure conditions. Average DAP was 13.5 Gy.cm<sup>2</sup> (6.8-23.9) for diagnostic and 66.8 Gy.cm<sup>2</sup> (28.7-108.5) for therapeutic ERCP ( $p < 0.05$ ). Average fluoroscopy time was 2.3 minutes (1.1-5.3) for diagnostic and 10.5 minutes (5.9-16.6) for therapeutic ERCP ( $p < 0.05$ ). DAP showed a linear relationship with fluoroscopy time ( $R^2 = 0.928$ ). Mean number of diagnostic and therapeutic films was 2.8 and 3.7, respectively. Fluoroscopic exposure represented 69% of the DAP for diagnostic ERCP and 90% of the DAP for therapeutic ERCP. Average ED was 3.1 mSv for diagnostic and 12.4 mSv for therapeutic ERCP. Therapeutic ERCP is associated with significantly higher radiation exposure than diagnostic ERCP. ED in therapeutic ERCP is a result largely of fluoroscopy time as opposed to number of films.

Ferreira LEVVC, Baron TH [9] studied the comparison of safety and efficacy of ERCP performed with the patients in supine and prone positions. In a retrospective study of 649 patients, (506 prone, 143 supine) undergoing ERCP by one endoscopist, success and complication rates were similar for both supine and prone patients (90.2%

and 11.2% for supine and 92.5% and 9.1% for prone, respectively), although the degree of procedural difficulty was significantly higher in the supine group.

Sornjarod O et al. [10] studied the radiation dose to medical staff in interventional radiology. The purposes of the study were to determine the dose to medical staff in interventional radiology at different locations on the body measured by thermoluminescent dosimeter (TLD) and to relate the medical staff dose to patient dose measured by the dose-area product (DAP) meter. The study covered 42 patients in three interventional radiology procedures with three x-ray machines. TLD were stuck at eight positions on the radiologist's skin during the procedure. In addition, direct reading from the DAP meter placed in front of the collimator of the x-ray tube, was recorded to estimate the patient radiation dose. The surface dose to the primary radiologist showed maximum value at the left forearm of 407  $\mu\text{Gy}$ . The ratios between the maximum interventional radiologist surface dose and patient dose were 12.88  $\mu\text{Gy}$  per 10  $\text{Gy}\cdot\text{cm}^2$  for transarterial oily chemoembolization TOCE (Siemens Polystar), 22.58  $\mu\text{Gy}$  per 10  $\text{Gy}\cdot\text{cm}^2$  for transarterial oily chemoembolization TOCE (Siemens Neurostar), 148.29  $\mu\text{Gy}$  per 10  $\text{Gy}\cdot\text{cm}^2$  for percutaneous transhepatic biliary drainage PTBD (Siemens Polystar) and 100.46  $\mu\text{Gy}$  per 10  $\text{Gy}\cdot\text{cm}^2$  for endoscopic retrograde cholangiopancreatography ERCP (GE Advantx). The interventional radiologist surface dose can be estimated from the mentioned ratio if the patient dose is measured. This will help the radiologists to avoid receiving an excess dose during their work.

I. A. Tsalafoutas et al. [11] studied the radiation dose to patients from endoscopic retrograde cholangiopancreatography examinations and image quality considerations. The purpose of this investigation was to measure the dose-area product (DAP) and the other relevant dosimetric quantities in diagnostic and therapeutic endoscopic retrograde cholangiopancreatography (ERCP). Furthermore, the dependence of patient dose and image quality on the tube potential was investigated. A DAP meter was used for dose monitoring in seven diagnostic and 21 therapeutic ERCPs. For each ERCP the DAP meter readings, fluoroscopy time, number of radiographs and exposure data were recorded. From these data the fluoroscopy and radiography contributions to DAP, the entrance skin dose and the effective dose for each examination were estimated. For the investigation of the effect of tube potential on patient dose and image quality, a water phantom containing syringes filled with diluted contrast media was used. The average DAP was 13.7  $\text{Gy}\cdot\text{cm}^2$  in diagnostic and 41.8  $\text{Gy}\cdot\text{cm}^2$  in therapeutic ERCP whereas the average fluoroscopy times were 3.1 and 6.0 min respectively. DAP was strongly correlated to the fluoroscopy time. Measurements in the phantom showed that a good compromise between image quality and patient dose is obtained for tube potentials around 80 kV. Therapeutic ERCPs deliver on average higher doses to patients than diagnostic ERCPs. However, for a difficult diagnostic ERCP more patient exposure may be required than for a simple therapeutic ERCP.

## CHAPTER III

### RESEARCH METHODOLOGY

#### 3.1 Research design

This study is an observational research.

#### 3.2 Research design model

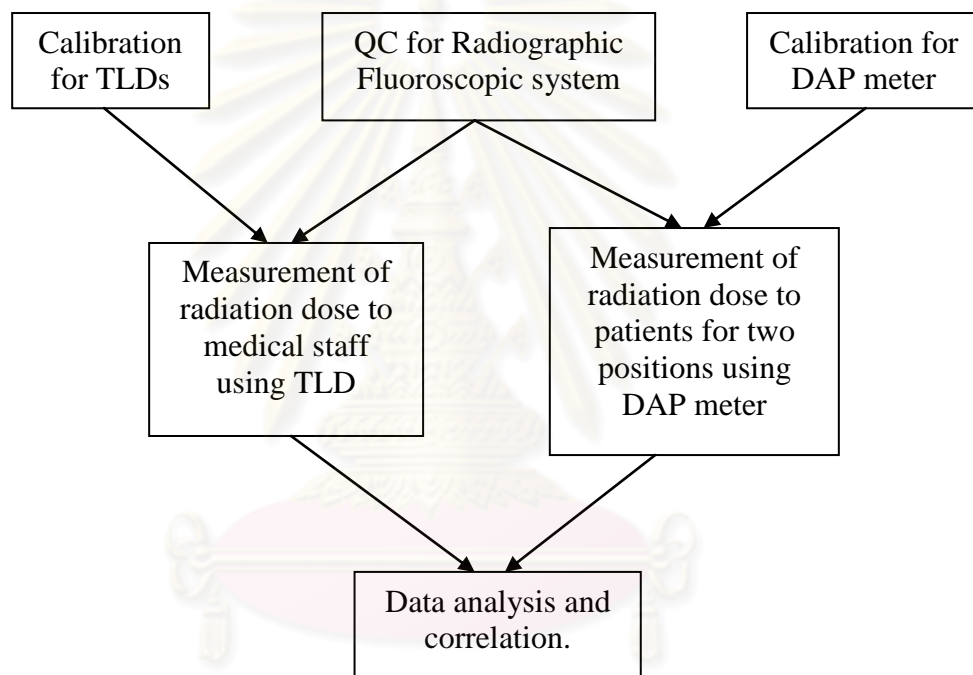


**Figure 3.1** The research design model

ศูนย์วิทยุทันตกรรม  
จุฬาลงกรณ์มหาวิทยาลัย



### 3.3 Conceptual framework

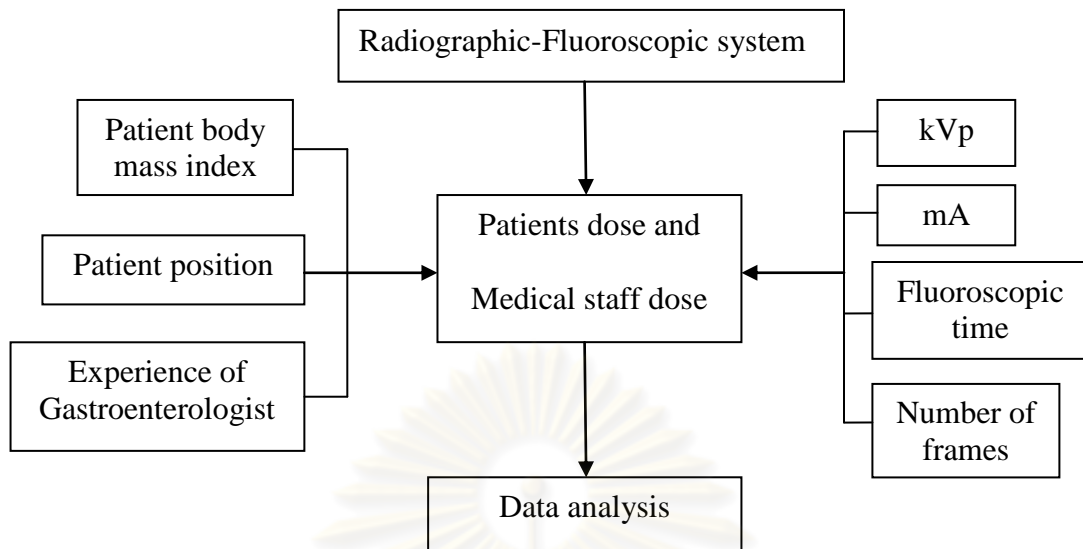


**Figure 3.2** Conceptual framework

### 3.4 Research questions

#### 3.4.1 Primary research question

What are the radiation dose in ERCP procedure to patients at two positions (prone and left lateral) and to medical staff?

#### 3.4.2 Secondary research question

What is the relationship between the patient doses for two patient positions using DAP meter and medical staff dose using TLD?

### 3.5 Key words

- Thermoluminescent dosimeter (TLD)
- Dose area product (DAP) meter
- Radiation dose
- Endoscopic Retrograde Cholangiopancreatography (ERCP)

### 3.6 The sample

#### 3.6.1 Target population

The patients and medical staff in ERCP procedure at Vascular and Interventional Radiology Unit, King Chulalongkorn Memorial Hospital.

#### 3.6.2 Sample population

Patients who underwent ERCP procedure at Vascular and Interventional Radiology Unit, King Chulalongkorn Memorial Hospital on Monday to Friday from period of July 2009 to January 2010, and met the eligible criteria.

#### 3.6.3 Eligible criteria

##### 3.6.3.1 Inclusion criteria

The patient positions are prone/left lateral all over the examination.

##### 3.6.3.2 Exclusion criteria

The patient who is not performed either prone or left lateral position during ERCP procedure.

#### 3.6.4 Sample size determination

Sample sizes for this study is calculated as two independent groups.

By formula:

$$n/group = 2(Z_{\alpha/2} + Z_{\beta})^2 \sigma^2 / (\bar{X}_1 - \bar{X}_2)^2$$

Define

$$\alpha = 0.05$$

$$\beta = 0.10$$

$$Z_{\alpha/2} = 1.96 \text{ (two tail)}$$

$$Z_{\beta} = 1.28$$

$$\bar{X}_1 = \text{Mean of patients dose in prone position during ERCP procedure.}$$

$$\bar{X}_2 = \text{Mean of patients dose in left lateral position during ERCP procedure.}$$

$$\sigma^2 = \text{Variance of doses in both data groups}$$

$$\sigma^2 = (n_1 - 1)S_1^2 + (n_2 - 1)S_2^2 / n_1 + n_2 - 2$$

$$n/group = 2(1.96 + 1.28)^2 (339.37) / (102.56 - 122.02)^2$$

$$n/group = 18.82 \approx 20$$

Sample size (n) for 95% confidence interval = 20 patients per group (2 groups)

### 3.7 Materials

#### 3.7.1 Radiographic-Fluoroscopic System

The x-ray machine for ERCP procedure is manufactured by Siemens Medical Solutions, model Polystar, installed in 1994.



**Figure 3.3** Radiographic-Fluoroscopic system, Siemens Medical Solutions, Model Polystar

#### 3.7.2 Unfors model Xi

A solid state radiation dosimeter with the read out device was used for QC of radiographic-fluoroscope machine as shown in figure 3.4.



**Figure 3.4** Unfors model Xi for QC of X-ray machines

### 3.7.3 Thermoluminescent dosimeter (TLD)

The TLD used in this study is lithium fluoride ( LiF ) crystal doped with magnesium and titanium ( LiF:Mg, Ti ). It is known as TLD-100. The nominal density of LiF is  $2.64 \text{ g/cm}^3$  and effective atomic number ( $z_{\text{eff}}$ ) of 8.2, the value closes to tissue. Thermoluminescent dosimeter chip with the dimension of  $3.2 \text{ mm} \times 3.2 \text{ mm} \times 0.89 \text{ mm}$  is shown in figure 3.5.

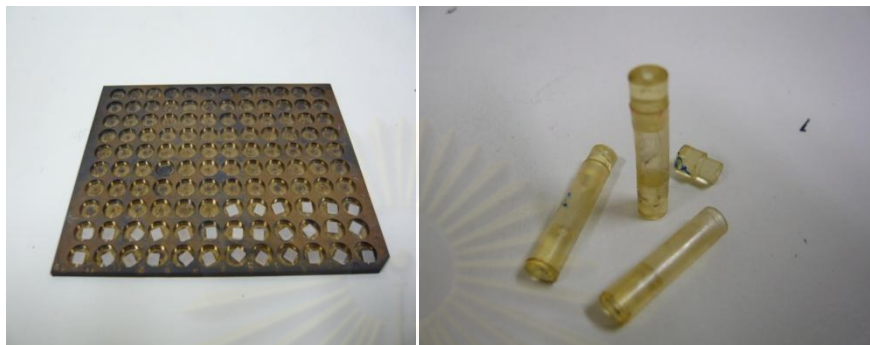


**Figure 3.5** Thermoluminescent dosimeter (TLD)

### 3.7.4 Automatic TLD reader

The Harshaw model 5500 automatic thermoluminescent dosimeter reader, is shown in figure 3.6. It is a personal computer driven, table-top instrument for TLD measurement. This reader is capable of reading 50 diameters per loading and accommodates TLD chips, rods and cubes in a variety of sizes. The reader uses nitrogen gas heating with a closed loop feedback system that produces linearly ramped temperatures accurate within  $\pm 1^\circ\text{C}$  to  $400^\circ\text{C}$ . Nitrogen is routed through the photomultiplier tube chamber to eliminate condensation.



**Figure 3.6** The Harshaw model 5500 automatic thermoluminescent dosimeter reader

### 3.7.5 DAP meter

The transmission ionization chamber model PTW-Diamentor E, is shown in figure 3.7. DAP meter is used to measure the dose in air (cGy), times the area of the x-ray field (cm<sup>2</sup>). The relationship between DAP and exposure-area product (EAP) is essentially a single conversion factor that relates dose to exposure. EAP is expressed in roentgen-cm<sup>2</sup> (R.cm<sup>2</sup>) and DAP is expressed in gray-cm<sup>2</sup> (Gy.cm<sup>2</sup>, usually read in cGy.cm<sup>2</sup>).

For recording the dose-area product, the flat transparent ionization chamber is fixed to the light beam diaphragm of the x-ray tube. This chamber is light-transparent and thus does not affect the routine use of the x-ray equipment.

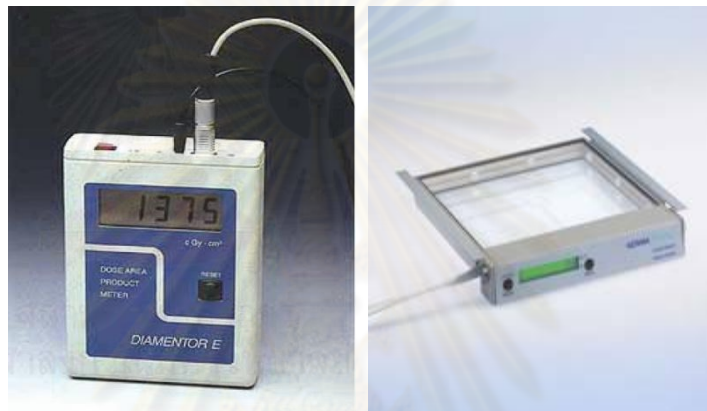


**Figure 3.7** Dose Area Product meter (DAP) model PTW-Diamentor E

### 3.7.6 Portal Film (Kodak portal pack for localization imaging)

The non screen ready packed film used for the radiation area verification.



**Figure 3.8** Film Kodak X – O Mat V

### 3.7.7 The patients

The patients underwent ERCP procedure at Vascular and Interventional Radiology Unit, King Chulalongkorn Memorial Hospital.



### 3.8 Methods

- 3.8.1 Perform the quality control of radiographic fluoroscopic system.
- 3.8.2 Calibrate DAP meter with ion chamber.
- 3.8.3 Calibrate thermoluminescent dosimeters (TLD).
- 3.8.4 Explain the procedure and rationale before place TLDs.
- 3.8.5 Place TLDs on medical staff at the left eye, under thyroid shield, left forearm, left leg, and lower abdomen of gastroenterologist and fellow, as shown in figure 3.9.

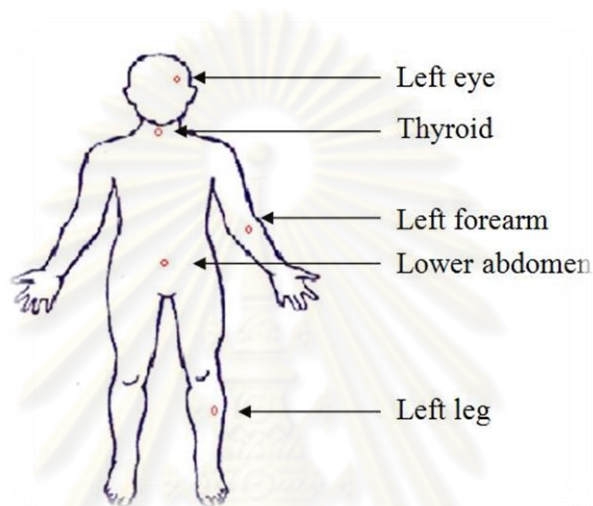


**Figure 3.9** TLDs placed on different sites on gastroenterologist.

- 3.8.6 Determine medical staff dose in ERCP procedure for each patient position with TLDs.
- 3.8.7 Place DAP in front of the collimator of x-ray tube. Place verification film on the couch at fluoroscopic area.
- 3.8.8 Exposed area will be determined by developed film.
- 3.8.9 At the end of ERCP procedure, record dose area product values in patient at two positions (prone and lateral).
- 3.8.10 Calculate average patient skin dose.
- 3.8.11 Relate patient dose ( $10 \text{ Gy.cm}^2$ ) at each patient position to medical staff dose ( $\mu\text{Gy}$ ).

### 3.9 Measurement

- Independent variables = patient position, kVp, mA, fluoroscopic time, number of frames, patient body mass index
- Dependent variables = patient dose and medical staff dose

### 3.10 Data collection

After the TLDs have been irradiated, they were read on the Harshaw model 5500 automatic TLD reader for thermoluminescent dosimetry method. Patient dose

was collected by DAP meter. Patient position, kVp, mA, fluoroscopic time, number of frame, patient body mass index were recorded in case record forms.

### **3.11 Data analysis**

#### **3.11.1 Summarization of Data**

Descriptive statistics : Mean, range and standard deviation (SD) of dose value.

Evaluation and comparison of result on two patient positions and medical staff in ERCP procedure.

Correlation between radiation doses of each patient position and medical staff.

#### **3.11.2 Data Presentation**

The table, bar chart and line graph are presented.

### **3.12 Expected benefits**

The radiation doses to patients and medical staff obtained from two patient positions were determined. The collected radiation dose were compared to the Dose Reference Level (DRL) for skin injury, in order to increase the awareness of radiation hazard to the patients and medical staff. In addition, the relationship between the dose received by medical staff and patients were performed and established. The aim of establishing such a relationship were able to identify the leading of higher personnel dose from the medical staff's technique and to provide suitable protective devices. The suitable position for patients and medical staff dose and success examination was obtained.

### **3.13 Ethical consideration**

Since, the measurement of radiation dose of ERCP procedure was directly performed in patients and medical staff at Vascular and Interventional Radiology Unit, King Chulalongkorn Memorial Hospital. Therefore, the ethical approval by the Ethic Committee of Faculty of Medicine, Chulalongkorn University was proceeded.

ศูนย์วิทยุทรัพยากร  
จุฬาลงกรณ์มหาวิทยาลัย

## CHAPTER IV

### RESULTS

#### 4.1 The quality control of Radiographic-Fluoroscopic System

The Radiographic-fluoroscopic system was calibrated for the following topics.

- Dose assessment
- Automatic brightness control test
- Table attenuation determination
- Maximum dose rate assessment
- Half value layer assessment
- Image quality assessment

The results on quality control of Radiographic-Fluoroscopic system were within acceptable range of IAEA CRP protocol (Appendix A)

#### 4.2 The data of patient studies

This study was recorded from forty patients who underwent ERCP procedures in twenty patients at prone position (12 female and 8 male) and twenty patients at left lateral position (8 female and 12 male). The average age was 64.25 (16-85) years, the patient height and weight were 159.95 (141-178) cm and 54.15 (30-78) kg at prone position as shown in table 4.1. Their average age was 62.15 (23-88) years, the patient height and weight were 165.05 (141-180) cm and 64.58 (35-95) kg at left lateral position as shown in table 4.2.

**Table 4.1** Patient data at prone position.

Case no.	Height (cm.)	Weight (kg.)	Sex	Age	Fluoro Time(min)	DAP (cGy.cm <sup>2</sup> )	ESD (mGy)	ESD (mGy/min)
1	161	57	M	67	7.35	1927	127.11	17.29
2	150	48	F	63	7.20	1582	70.02	9.73
3	151	45	F	83	6.58	1795	85.51	12.99
4	160	52	F	49	9.44	2145	95.55	10.12
5	173	76	M	77	5.34	1767	98.55	18.46
6	163	54	F	36	10.28	2109	99.09	9.64
7	154	38	F	16	3.37	710	39.76	11.80
8	165	66	M	63	5.15	1504	69.95	13.58
9	151	43	F	82	2.57	839	48.78	18.98
10	150	53	F	83	3.16	637	44.82	14.18
11	157	60	F	77	5.48	1356	57.42	10.48
12	171	78	M	85	9.02	1849	100.67	11.16
13	174	64	M	62	1.33	788	48.27	36.29
14	160	56	F	78	4.10	1176	67.79	16.53
15	159	62	F	59	14.27	3563	151.34	10.61

**Table 4.1** Patient data at prone position. (Continued)

Case no.	Height (cm.)	Weight (kg.)	Sex	Age	Fluoro Time(min)	DAP (cGy.cm <sup>2</sup> )	ESD (mGy)	ESD (mGy/min)
<b>16</b>	163	47	M	67	3.59	1632	84.81	23.62
<b>17</b>	160	45	M	38	5.37	1415	63.65	11.85
<b>18</b>	158	43	F	35	4.58	1570	67.95	14.84
<b>19</b>	141	30	F	84	5.43	1181	62.80	11.57
<b>20</b>	178	66	M	81	18.28	4101	174.74	9.56
<b>Average</b>	159.95	54.15		64.25	6.59	1682.30	82.93	14.66
<b>Min</b>	141	30	M=8	16	1.33	637	39.76	9.56
<b>Max</b>	178	78	F=12	85	18.28	4101	174.74	36.29

**Table 4.2** Patient data at left lateral position.

Case no.	Height (cm.)	Weight (kg.)	Sex	Age	Fluoro Time(min)	DAP (cGy.cm <sup>2</sup> )	ESD (mGy)	ESD (mGy/min)
<b>1</b>	150	55	F	62	7.51	2487	122.74	16.34
<b>2</b>	178	95	M	74	4.57	2981	176.29	38.58
<b>3</b>	173	75	M	77	2.24	820	52.33	23.36
<b>4</b>	178	83.5	M	23	3.06	1857	123.08	40.22
<b>5</b>	160	45	F	38	5.26	5367	224.50	42.68
<b>6</b>	170	68	M	88	6.54	2245	105.12	16.07
<b>7</b>	165	58	M	73	2.58	923	60.02	23.26
<b>8</b>	160	44	M	58	1.00	343	23.30	23.30
<b>9</b>	141	35	F	84	5.56	823	50.41	9.07
<b>10</b>	173	60	M	85	20.00	4745	187.61	9.38
<b>11</b>	180	85	M	87	6.45	3018	134.00	20.78
<b>12</b>	162	70	M	80	18.02	5766	229.30	12.72
<b>13</b>	165	71	F	57	4.50	4201	168.53	37.45
<b>14</b>	173	81	M	51	2.49	2174	104.66	42.03
<b>15</b>	167	73	F	30	4.11	1020	50.16	12.20
<b>16</b>	165	69	M	54	1.20	540	31.93	26.61
<b>17</b>	163	59	M	51	4.22	1187	68.43	16.22
<b>18</b>	161	65	F	35	3.50	1224	74.64	21.33
<b>19</b>	156	37	F	53	4.26	590	33.73	7.92
<b>20</b>	161	63	F	83	3.41	1396	67.20	19.71
<b>Average</b>	165.05	64.58		62.15	5.52	2185.35	124.06	22.96
<b>Min</b>	141	35	M=12	23	1.00	343	23.30	7.92
<b>Max</b>	180	95	F=8	88	20.00	5766	229.30	42.68

### 4.3 Thermoluminescent dosimeter calibration

#### 4.3.1 Sensitivity of TLD-100 chips

The relative sensitivity of these TLD chips was determined and individual calibration factors were calibrated. The sensitivity or the element correction coefficient factors (ECC) of individual TLD chip ranged from 0.902 to 1.072 for the TLD chips that were used in this study. Only the TLD chips which had the sensitivity factor close to 1.0(0.99 to 1.01) was selected in the calibration of reader calibration factor (RCF) by equation 2.3.

#### 4.3.2 Linearity of TLD-100 chips

The linearity of TLD-100 chips response was studied by irradiated TLD-100 chips in air at absorbed dose of known dose at 80 kVp and 100 kVp. The charge corrected by the sensitivity was plotted with the absorbed dose range from 30 to 700  $\mu\text{Gy}$ . They are shown in figure 4.1 and 4.2 for 80 kVp and 100 kVp respectively. The graph showed the linear relationship between TLDs and absorbed dose responses with the correlation coefficient of 0.995-0.9984.

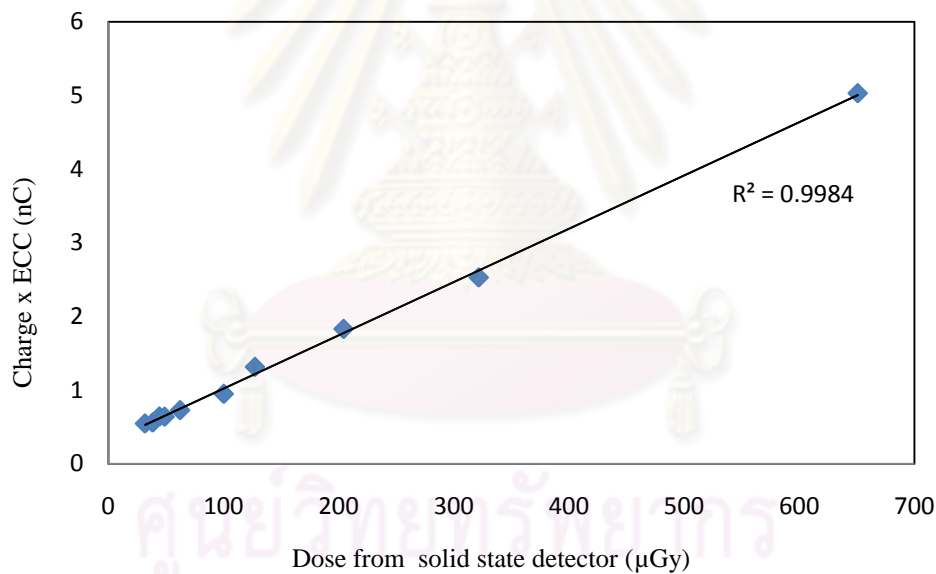


**Figure 4.1** Linearity of LiF TLD-100 when irradiated at various doses for 80 kVp.



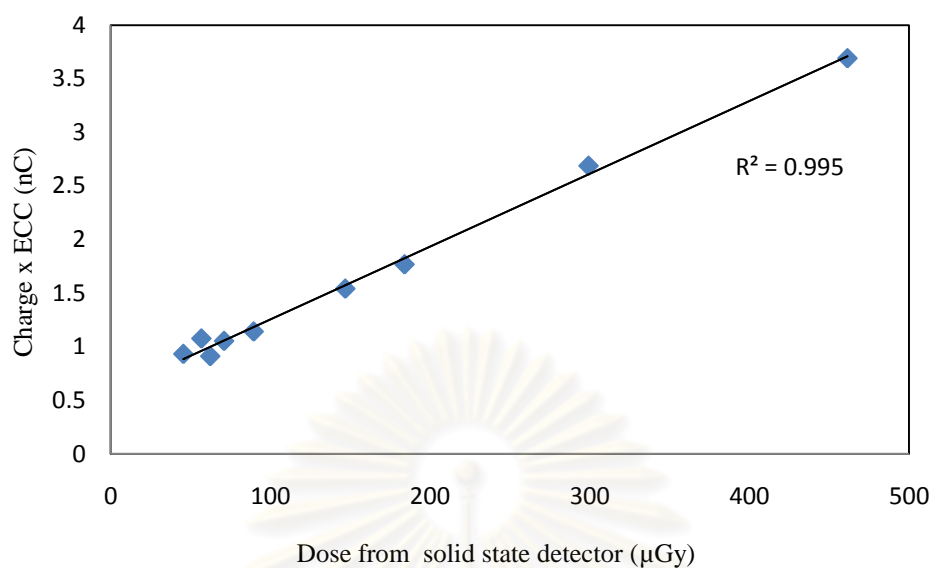


**Figure 4.2** Linearity of LiF TLD-100 when irradiated at various doses for 100 kVp.

#### 4.3.3 Minimum detectable dose

The characteristic of thermoluminescent dosimeter including variation coefficient (VC) of some dose values, background (BG) and minimum detectable dose (MDD) are reported in table 4.3. The calculated value of MDD was 14.8 µGy by using equation 4.1.

$$MDD=3\times VC\times BG \quad (4.1)$$

**Table 4.3** Reading values of background.

No.	Reading values (µGy)
1	28.5
2	20.4
3	24.2
4	19.7
5	33.7
6	29.0
7	29.7
8	30.7
9	22.6
<b>Mean</b>	26.5
<b>SD</b>	4.9
<b>VC=SD/BG</b>	0.185

#### 4.4 Measurement of radiation dose in medical staff

##### 4.4.1 Patients prone positions.

##### 4.4.1.1 The radiation doses to the first medical staff

Table 4.4 shows the results from the dose received by the first medical staff in ERCP procedure at patient prone position range from 0.62 to 382.81  $\mu\text{Gy}$ . The lowest dose value, close to background, at the lower abdomen in lead apron is 0.62  $\mu\text{Gy}$  and the highest dose value at the left forearm of 382.81  $\mu\text{Gy}$ .

**Table 4.4** The radiation dose to the first medical staff at patient prone position, measured by TLD-100.

TLD location	Sample size	Average ( $\mu\text{Gy}$ )	Range ( $\mu\text{Gy}$ )
Left eye	20	58.85	8.25 - 178.62
Thyroid	20	68.39	2.52 - 244.95
Lower abdomen	20	16.45	0.62 - 75.49
Left forearm	20	131.09	29.90 - 382.81
Left leg	20	48.34	9.07 - 126.83

##### 4.4.1.2 The radiation doses to the second medical staff

Table 4.5 shows the results from TLD-100 in ERCP procedure at patient prone position. The radiation doses to the second medical staff range from 0.50 and 253.83  $\mu\text{Gy}$ . The lowest dose value, close to background, at the lower abdomen in lead apron is 0.50  $\mu\text{Gy}$  and the highest dose value at the left forearm is 253.83  $\mu\text{Gy}$ .

**Table 4.5** The radiation dose to the second medical staff per ERCP procedure to patients at prone positions, measured by TLD-100.

TLD location	Sample size	Average ( $\mu\text{Gy}$ )	Range ( $\mu\text{Gy}$ )
Left eye	20	40.06	5.49 – 114.09
Thyroid	20	47.98	2.01 – 118.47
Lower abdomen	20	12.67	0.50 – 71.34
Left forearm	20	77.04	4.55 – 253.83
Left leg	20	31.44	3.08 – 101.06

#### 4.4.2 Patients left lateral positions.

##### 4.4.2.1 The radiation doses to the first medical staff

Table 4.6 shows the results from TLD-100 in ERCP procedure to the first medical staff range from 0.50 and 1628.66  $\mu\text{Gy}$  for patient left lateral position. The lowest dose value, close to background, at the lower abdomen in lead apron is 0.50  $\mu\text{Gy}$  and the highest dose value at the left forearm is 1628.66  $\mu\text{Gy}$ .

**Table 4.6** The radiation dose to the first medical staff per ERCP procedure at patient left lateral position, measured by TLD-100.

TLD location	Sample size	Average ( $\mu\text{Gy}$ )	Range ( $\mu\text{Gy}$ )
Left eye	20	84.14	32.20 - 180.82
Thyroid	20	77.37	12.39 - 172.44
Lower abdomen	20	48.37	0.50 - 101.60
Left forearm	20	244.02	54.79 - 1628.66
Left leg	20	85.59	6.99 - 202.57

##### 4.4.2.2 The radiation doses to the second medical staff

Table 4.7 shows results from TLD-100 procedure at patient left lateral position. The radiation dose to the second medical staff range from 2.40 and 389.74  $\mu\text{Gy}$ . The lowest dose value, close to background, at the lower abdomen in lead apron is 2.40  $\mu\text{Gy}$  and the highest dose value at the left forearm is 389.74  $\mu\text{Gy}$ .

**Table 4.7** The radiation dose to the second medical staff at patient left lateral position, measured by TLD-100.

TLD location	Sample size	Average ( $\mu\text{Gy}$ )	Range ( $\mu\text{Gy}$ )
Left eye	20	79.15	20.84 - 188.99
Thyroid	20	87.33	9.51 - 194.96
Lower abdomen	20	41.80	2.40 - 100.08
Left forearm	20	124.26	13.75 - 389.74
Left leg	20	82.91	15.71 - 164.50

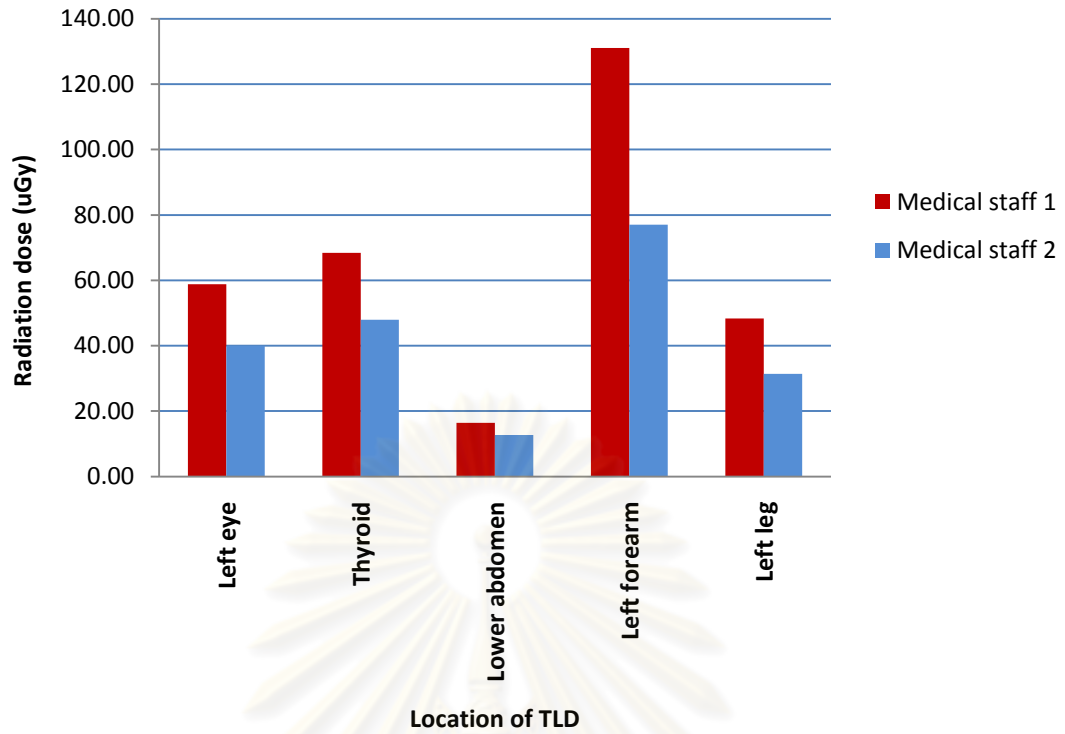


**Figure 4.3** The average doses ( $\mu\text{Gy}$ ) to the first and second medical staff at patient prone position.

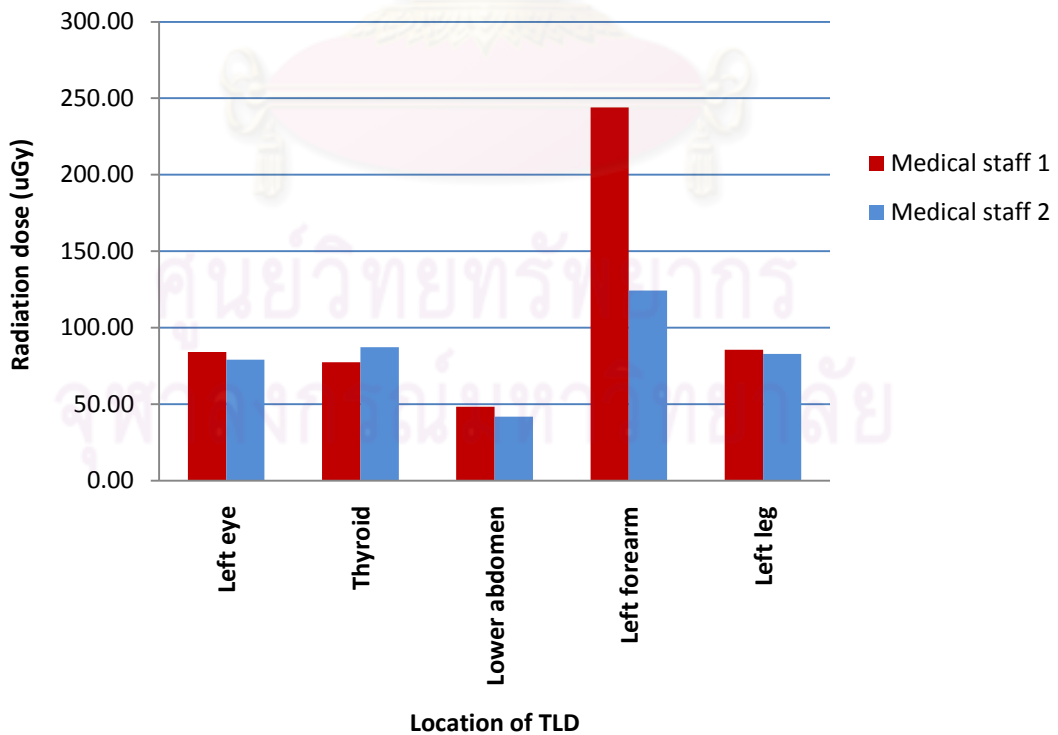


**Figure 4.4** The average doses ( $\mu\text{Gy}$ ) to the first and second medical staff at patient left lateral position.

These data were plotted to show the average dose at five locations of the first and the second medical staff, as in figure 4.3 and 4.4. The bar charts show the different dose between the first and the second medical staff of patient at two positions (prone and left lateral). This is due to the fact that the first medical staff stands at about 40-60 cm from the X-ray tube, whereas for the second medical staff was about 80-120 cm. The average dose difference between the first and the second medical staff is 41.23 % of patient prone position and 49.10% of patient left lateral position.

The results of the average dose for the first and the second medical staff at patient two positions (prone and left lateral) are shown in figure 4.5 and 4.6. The first and the second medical staff received the maximum dose per procedure at the left forearm of both positions. The average dose at left lateral position was higher than prone position.

#### **4.5 Measurement of dose-area product in patient**

The results of dose-area product and the average dose to patient during ERCP procedures at two positions (prone and left lateral) are shown in table 4.1 and 4.2. The average dose-area product was 1682.30(637-4101) cGy.cm<sup>2</sup> per procedure, the average fluoroscopic time was 6.59 (1.33-18.28) minutes and the average skin dose from DAP was 82.93(39.76-174.74) mGy, for prone position. The average dose-area product was 2185.35(343-5766) cGy.cm<sup>2</sup> per procedure, the average fluoroscopic time was 5.52 (1.00-20.00) minutes and the average skin dose from DAP was 124.06(23.730-229.30) mGy, for left lateral position.

From table 4.1 and 4.2 the patient dose between the prone and left lateral position at 95% confidence interval, this difference is considered to be very statistically significant ( $p < 0.05$ ).



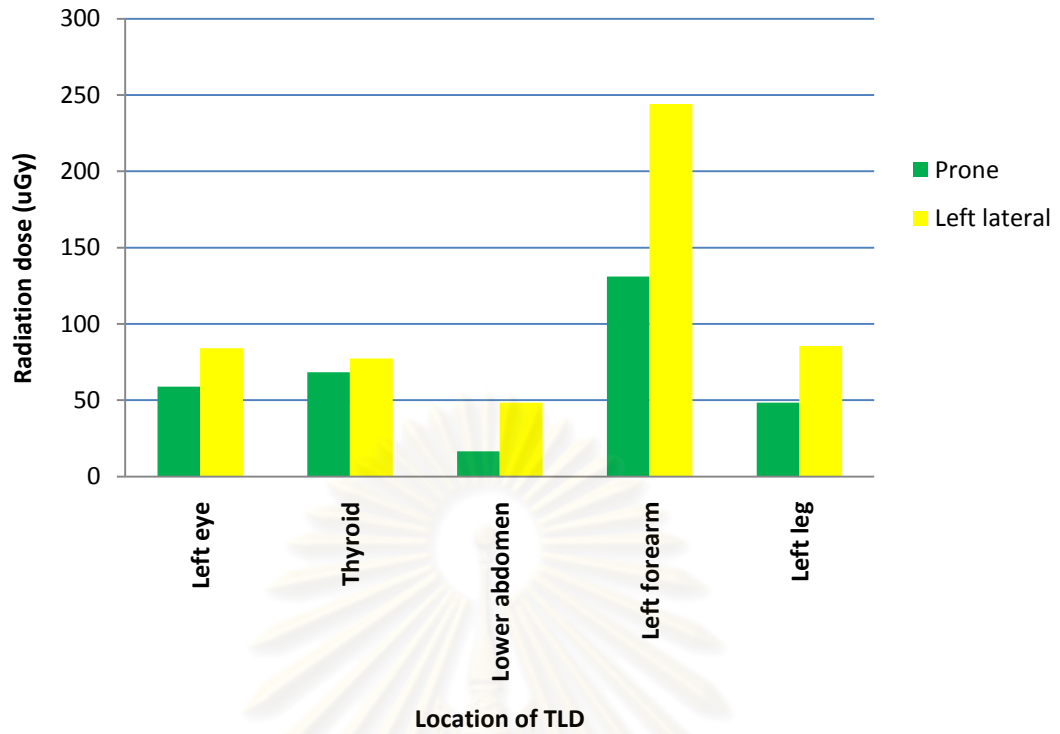


**Figure 4.5** The average doses ( $\mu\text{Gy}$ ) to the first medical staff at two positions.

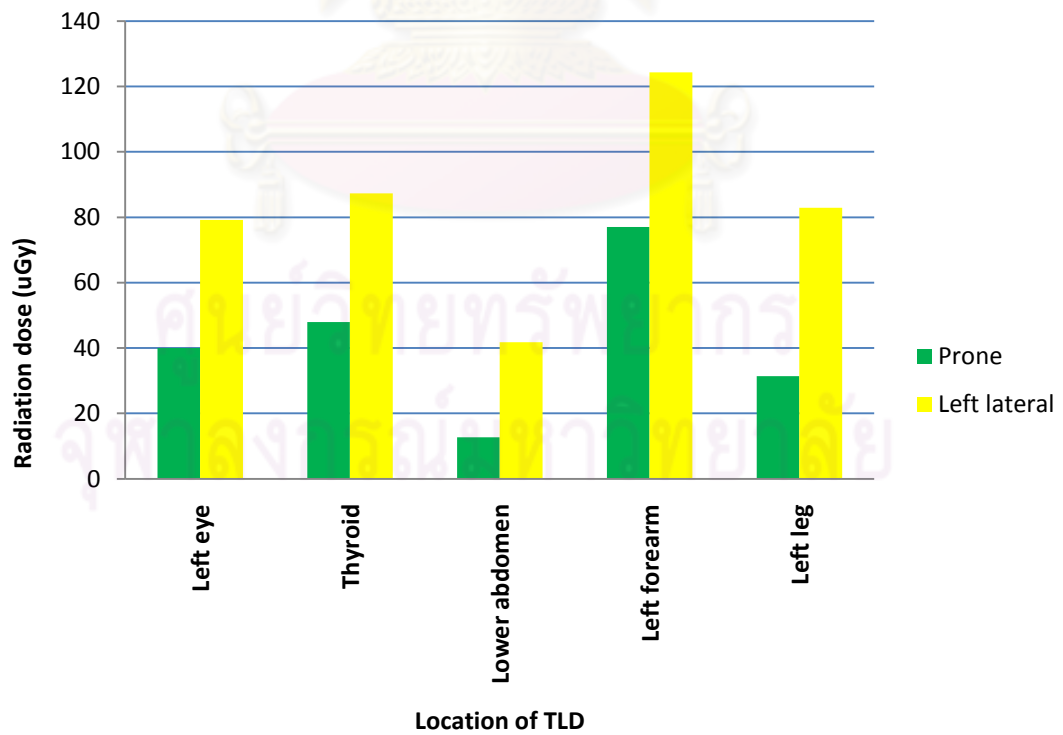


**Figure 4.6** The average doses ( $\mu\text{Gy}$ ) to the second medical staff at two positions.

#### 4.6 The Relationship between the patient dose and medical staff dose

The scatter plot shows the relationship between the patient dose ( $\text{cGy}\cdot\text{cm}^2$ ) at prone position and dose at left forearm of the first and second medical staff to the most exposed per procedure from ERCP. The correlation between the patient dose at prone position and dose at left forearm of the both medical staff are poor correlation  $R=0.19$  and  $R=0.38$ . These relationships are shown in figure 4.7 and 4.8, respectively.

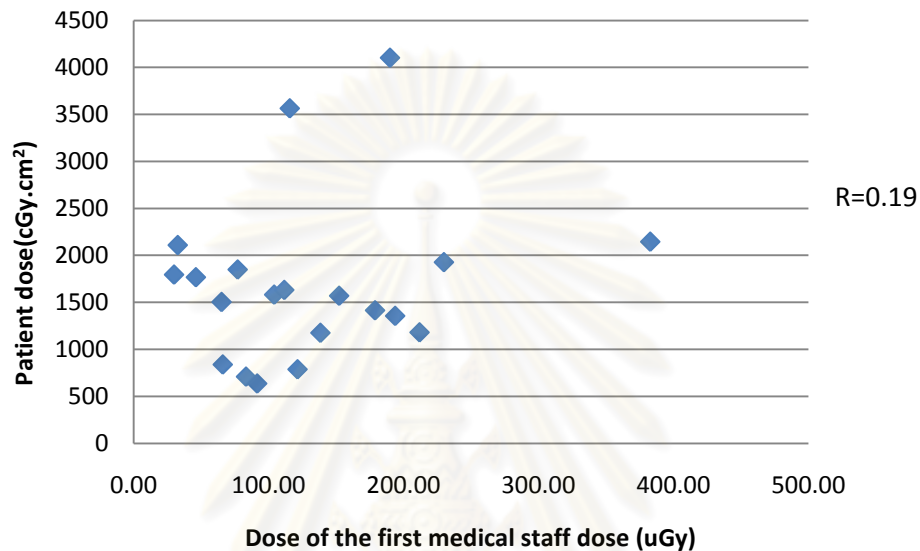


**Figure 4.7** The relation between patient doses ( $\text{cGy}\cdot\text{cm}^2$ ) at prone position and dose to left forearm of the first medical staff ( $\mu\text{Gy}$ )

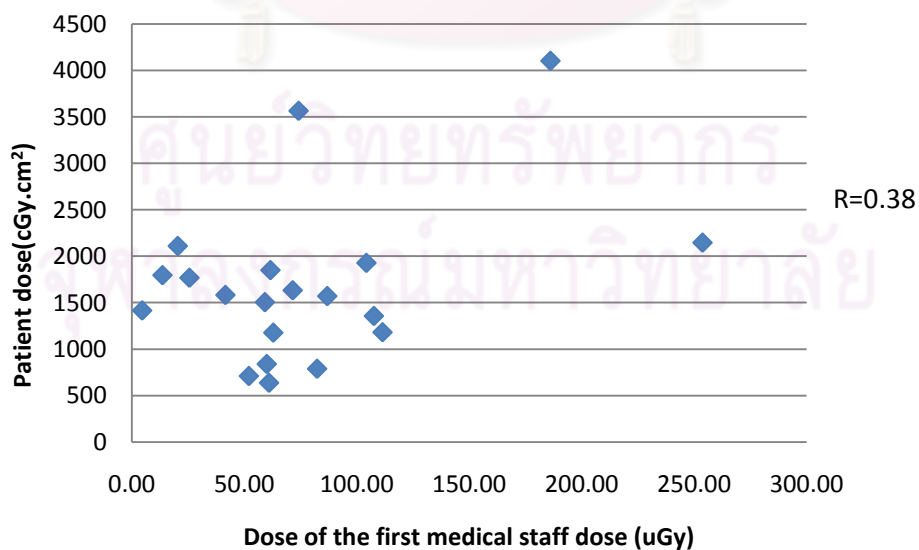


**Figure 4.8** The relation between patient doses ( $\text{cGy}\cdot\text{cm}^2$ ) at prone position and dose to left forearm of the second medical staff ( $\mu\text{Gy}$ )

The scatter plot show the relationship between the patient dose ( $\text{cGy}\cdot\text{cm}^2$ ) at left lateral position and dose at left forearm of the first and second medical staff to the most exposed per procedure from ERCP. The correlation between the patient dose at left lateral position and dose at left forearm of the both medical staff are poor correlation  $R=0.43$  and  $R=0.35$ . These relationships are shown in figure 4.9 and 4.10, respectively.

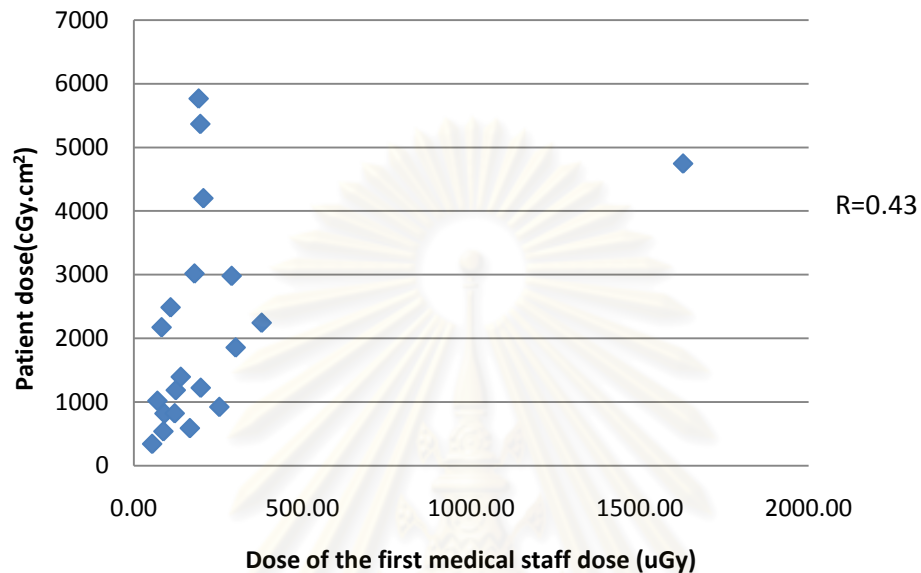


**Figure 4.9** The relation between patient doses ( $\text{cGy}\cdot\text{cm}^2$ ) at left lateral position and dose to left forearm of the first medical staff ( $\mu\text{Gy}$ )

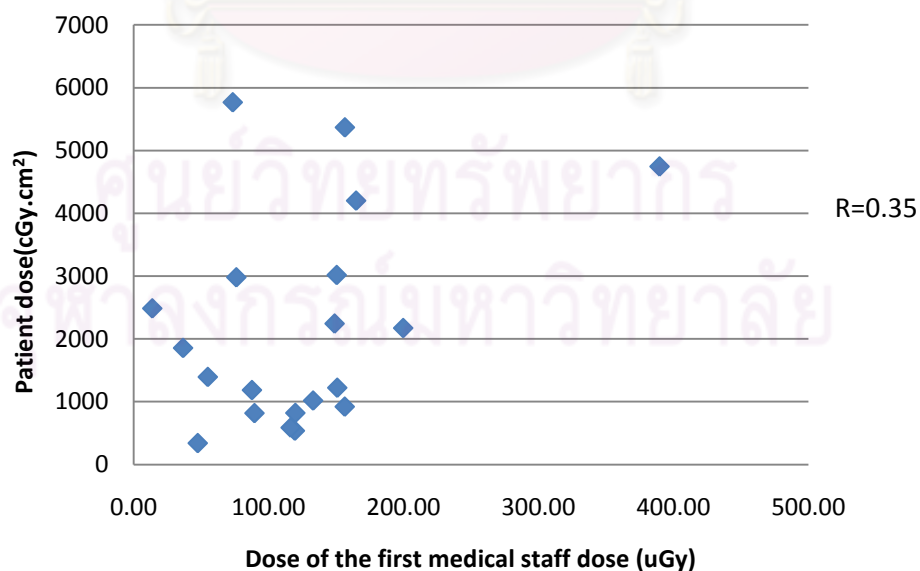


**Figure 4.10** The relation between patient doses ( $\text{cGy}\cdot\text{cm}^2$ ) at left lateral position and dose to left forearm of the second medical staff ( $\mu\text{Gy}$ )

**Table 4.8** The ratio of averaged values between occupational doses and dose-area product in  $\mu\text{Gy} / 10 \text{ Gy}\cdot\text{cm}^2$  from TLD reading at five locations on medical staff and from DAP.

Location	ERCP ( $\mu\text{Gy} / 10 \text{ Gy}\cdot\text{cm}^2$ )	
	First medical staff	Second medical staff
<b>Prone position</b>		
Left eye	34.98	23.81
Thyroid	40.65	28.52
Lower abdomen	9.78	7.53
Left forearm	77.92	45.79
Left leg	28.73	18.45
<b>Left lateral position</b>		
Left eye	38.50	36.22
Thyroid	35.40	39.96
Lower abdomen	22.13	19.13
Left forearm	111.66	56.86
Left leg	39.16	37.94

The relation between occupational doses from TLD and patient doses evaluated from the dose-area product was established and shown in table 4.8. For five locations of the body (left eye, thyroid, lower abdomen, left forearm and left leg), the highest ratio between average occupational doses and dose-area product is the left forearm and the lowest ratio is the lower abdomen of ERCP procedure. The highest ratio is  $111.66 \mu\text{Gy} / 10 \text{ Gy}\cdot\text{cm}^2$  and the lowest ratio is  $7.53 \mu\text{Gy} / 10 \text{ Gy}\cdot\text{cm}^2$ . Considering the 2 techniques, the ratio between average occupational doses and dose-area product of left lateral position show higher value than prone position.

ศูนย์วิทยุทรัพยากร  
จุฬาลงกรณ์มหาวิทยาลัย

## CHAPTER V

### DISCUSSION AND CONCLUSION

#### 5.1 Discussion

The sensitivity, linearity and minimum detectable dose of TLDs were determined before the measurement of free air exposure the radiographic-fluoroscopic system at 80 and 100 kVp. The sensitivity range of TLD-100 was 0.901 to 1.072 which agree with Phakamart T [12], et al with the sensitivity range from 0.924 to 1.072. The minimum detectable dose was 0.016  $\mu\text{Gy}$  which mean that the doses lower than this value could not be measured. The relation between TLDs response and dose at energy of 80 and 100 kVp was shown at the good linearity with the correlation coefficient at 0.998 and 0.995, respectively. So, any level of absorbed doses could be measured by this set of TLDs.

The DAP read outs had been compared to DRL(diagnostic reference level) values derived from data collected in the UK(United Kingdom).[13]

**Table 5.1** DAP values from this study and DRL (UK).

Examination	DRL(UK)	This study	
	Prone	Prone	Left lateral
ERCP	19.0 Gy.cm <sup>2</sup>	16.82 Gy.cm <sup>2</sup>	21.85 Gy.cm <sup>2</sup>

From table 5.1, the DAP read out from ERCP procedure was 16.82 Gy.cm<sup>2</sup> at prone position and 21.85 Gy.cm<sup>2</sup> at left lateral position. DRL from UK, the DAP value is 19 Gy.cm<sup>2</sup>.

The average surface dose the patient received at prone and left lateral positions were 82.93 and 124.06 mGy per procedure and lower than the skin injury level of 2 Gy. The medical staff was adequately protected from the risk of working with the radiation. The medical staff dose can be estimated from the patient dose using DAP method. This will help the medical staff avoid the excess dose during their work.

The ratio between average occupational doses and dose-area product in the ERCP procedure at the lower abdomen, left forearm and left leg are 9.78, 77.72 and 28.73  $\mu\text{Sv}/10 \text{ Gy.cm}^2$ , respectively. The results can be compared with Sornjarod O [8], et al who derived the average value of the ratio between occupational doses and dose-area product at the lower abdomen, left forearm and left leg of 1.26, 100.46 and 81.91  $\mu\text{Sv}/10 \text{ Gy.cm}^2$ , respectively.



In this study DAP measurements during therapeutic ERCP values of 16.8 Gy.cm<sup>2</sup> from patient prone position and 21.9 Gy.cm<sup>2</sup> from patient left lateral position. From table 5.2, the average DAP are lower than the corresponding values of 66.8 and 41.8 Gy.cm<sup>2</sup> by Larkin C.J.[8] and I. A. Tsalafoutas [11], respectively.

**Table 5.2** Average DAP for therapeutic ERCP

ERCP / Country	Average DAP (Gy.cm <sup>2</sup> )
<b>Northern Ireland</b>	66.8
<b>Greece</b>	41.8
<b>This study</b>	
-Prone	16.8
-Left lateral	21.9

From table 5.3 show the annual dose the first medical staff received from ERCP at the left forearm of 52.4 mSv per year from patient prone position and 97.6 mSv per year from patient left lateral position.

From table 5.4 show the annual dose the second medical staff at the left forearm of 52.4 mSv per year from patient prone position and 97.6 mSv per year from patient left lateral position.

**Table 5.3** Calculation of the first medical staff dose per year at different organs from ERCP procedure.

Location	Cases / year	Average dose / case (mSv)	Dose limit (mSv) / year	Dose / Case/year (mSv)	Dose / Case/day (μSv)
<b>Prone position</b>					
Left eye	400	0.058	150	23.2	92.8
Thyroid	400	0.068	-	27.2	108.8
Lower abdomen	400	0.016	150	6.4	25.6
Left forearm	400	0.131	500	52.4	209.6
Left leg	400	0.048	500	19.2	76.8
<b>Left lateral position</b>					
Left eye	400	0.084	150	33.6	134.4
Thyroid	400	0.077	-	30.8	123.2
Lower abdomen	400	0.048	150	19.2	76.8
Left forearm	400	0.244	500	97.6	390.4
Left leg	400	0.085	500	34.0	136.0

**Table 5.4** Calculation of the second medical staff dose per year at different organs from ERCP procedure.

Location	Cases / year	Average dose / case (mSv)	Dose limit (mSv) / year	Dose / Case/year (mSv)	Dose / Case/day ( $\mu$ Sv)
<b>Prone position</b>					
Left eye	400	0.040	150	16.0	64.0
Thyroid	400	0.047	-	18.8	75.2
Lower abdomen	400	0.012	150	4.8	19.2
Left forearm	400	0.077	500	30.8	123.2
Left leg	400	0.031	500	12.4	49.6
<b>Left lateral position</b>					
Left eye	400	0.079	150	31.6	126.4
Thyroid	400	0.087	-	34.8	139.2
Lower abdomen	400	0.041	150	16.4	65.6
Left forearm	400	0.124	500	49.6	198.4
Left leg	400	0.082	500	32.8	131.2

Although this is lower than the dose limit, but the relationship between the dose relieved by medical staff and patients will also be performed and established. The aim of establishing such a relationship will be able to identify the leading of higher personnel dose from the medical staff's technique and to provide suitable protective devices.

## 5.2 Conclusion

This study includes forty patients who underwent ERCP procedures in twenty patients at prone position and twenty patients at left lateral position. The relationship between the medical staff dose determined by TLD and the patient dose by DAP is poor, while the first medical staff received the maximum dose per procedure at the left forearm of 244.02 (54.79-1628.66)  $\mu$ Gy for patient at left lateral position and 131.09 (29.90-382.81)  $\mu$ Gy at prone position.

In addition, the patient received the maximum dose per procedure at left lateral position and the first medical staff received the radiation dose per procedure higher than the second medical staff at patient both position (prone and left later position).

## 5.3 Recommendation

In this study, the awareness of the medical staff of patient dose, optimize the patient position and the dose settings of the x-ray units in this specialty are recommended

## REFERENCES

- [1] Khan FM. The physics of Radiation Therapy. 3<sup>rd</sup> ed. USA: Lippincott Williams & Wilkins, 2003.
- [2] Cameron JR, Suntharalingam N, Kenney GN. Thermoluminescent dosimetry. Milwaukee. The University of Wisconsin Press, 1968.
- [3] Harshaw Bicon radiation measurement produced. Model 5500 automatic TLD reader user's manual. Ohio : Saint - Gobian / Norton industrial ceramics, 1993.
- [4] International Atomic Energy Agency. Dosimetry in diagnostic radiology:An international code of practice. IAEA TRS 457, Austria. 2007.
- [5] International Commission on Radiation Units and Measurements. Quantities and units in radiation protection dosimetry. ICRU Report 51 (Bethesda, MD: ICRU), 1993.
- [6] International Commission on Radiological Protection (ICRP Publication No. 103), Centre for Radiation, Chemical and Environmental Hazards, Health Protection Agency (HPA). 2007
- [7] United Kingdom Accreditation Service (UKAS). The expression of uncertainty and confidence in measurement. UKAS Publication Ref:LAB 12(2000):1-13.
- [8] Larkin C.J. et al. Radiation doses to patient during ERCP. GASTROINTESTINAL ENDOSCOPY 53(2001):161-164.
- [9] Ferreira LEVVC, Baron TH. Comparison of safety and efficacy of ERCP performed with the patient in supine and prone positions. GASTROINTESTINAL ENDOSCOPY 67(2008):1037-1043.
- [10] Sornjarod Oonsiri, Chotika Jumpangern, Taweap Sanghangthum, Anchali Krisanachinda, Sivalee Suriyapee. Radiation Dose to Medical Staff in Interventional Radiology. Journal of the Medical Association of Thailand 90 (2007):823-828.
- [11] I. A. Tsalafoutas et al. the radiation dose to patients from endoscopic retrograde cholangiopancreatograph examinations and image quality considerations. Radiation Protection Dosimetry 106 (2003):241-246.
- [12] Thaoyabut P. Fetal dose in rando phantom from computed radiography of abdomen, pelvis and lumbo-sacral spine. Master's Thesis, Science Program in Medical Imaging Faculty of Medicine Chulalongkorn University, 2007.

- [13] The Medical Council Regulates the Medical Profession in Ireland. Diagnostic Reference Levels Position Paper , 2004.



ศูนย์วิทยทรัพยากร  
จุฬาลงกรณ์มหาวิทยาลัย



**APPENDICES**

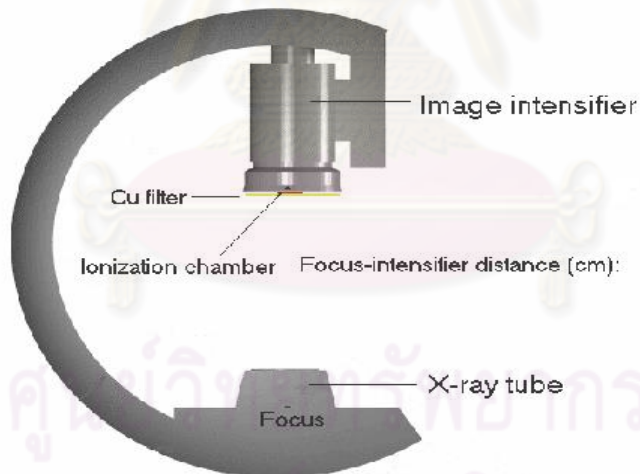
ศูนย์วิทยทรัพยากร  
จุฬาลงกรณ์มหาวิทยาลัย



**APPENDIX A**  
**EQUIPMENT PERFORMANCE FOR FLUOROSCOPY EQUIPMENT**

<b>Hospital :</b>	King Chulalongkorn Memorial Hospital
<b>X-ray Unit :</b>	Siemens Polystar
<b>Room :</b>	No.2 Narathip Building Ground Floor
<b>Report Number :</b>	1.0
<b>Date :</b>	Mar 21, 2009
<b>Test performed by :</b>	Wachirapong Suwanboonrit

Antiscatter grid not removed  
Single plane



## DOSE ASSESSMENT

Focus-Intensifier detector (cm.) 100 cm.

Patient dose measurement: Focus-Patient distance 60 cm.

Entrance Image Intensifier dose measurement: Focus-Ion chamber distance 45.6 cm.

Mode	Submode/ Image quality	Pulse rate (pulses/s)	Automatic added filtration (mmCu)	Field size (cm)	kV	mA	Added Filtration (mm Cu)	(Patient entrance surface air kerma) Copper filter entrance air kerma ( $\mu\text{Gy/s}$ )	Image Intensifier entrance air kerma (mGy/min)	Patient entrance surface air kerma at 70 cm (including backscatter)	Phantom
Fluoro 1		Cont	2	40	78	0.8	2.0	46.77			2mm Cu
				28	79	0.9		51.58			
				20	84	1.0		75.06			
				14	91	1.3		117.00			
Fluoro 2				40	70	2.7		108.00			2mm Cu
				28	70	3.2		114.90			
				20	70	6.2		229.60			
				14	76	5.7		275.70			
Fluoro 3				40	71	1.9		196.70			2mm Cu
				28	71	2.1		201.80			
				20	74	2.8		290.50			
				14	77	3.8		436.80			

จุฬาลงกรณ์มหาวิทยาลัย

**DOSE ASSESSMENT**

Mode	Submode/ Image quality	Pulse rate (pulses/s)	Automatic added filtration (mmCu)	Field size (cm)	kV	mA	Added Filtration (mm Cu)	(Patient entrance surface air kerma) Copper filter entrance air kerma ( $\mu$ Gy/s)	Image Intensifier entrance air kerma (mGy/min)	Patient entrance surface air kerma at 70 cm (including backscatter)	Phantom
Turbo		15p/s	2	40	77	3.9	2.0	842.3			2mm Cu
				28	77	3.9		841.8			
				20	77	3.9		823.5			
				14	77	3.9		819.3			
Single shot				40	87.5	3.9		2364.0			
Fluoro 1				28	87.5	3.9		2715.0			
				20	87.5	3.9		6517.0			
				14	87.5	3.9		10110.0			

ศูนย์วิทยุทรัพยากร  
จุฬาลงกรณ์มหาวิทยาลัย

### AUTOMATIC BRIGHTNESS CONTROL TEST

FID 100 cm

Mode	Submode/ Image quality	Pulse rate (pulses/s)	Automatic added filtration (mmCu)	Field size (cm)	Pulse with (ms)	Dose rate ( $\mu$ Gy/s)	kV	mA
Fluoro 1	Normal mode	Continuous	1.0	20		133.2	72	0.7
			2.0	20		136.8	82	1.0
			3.0	20		151.6	91	1.3

\*Only one mode and field size is checked (about 20 cm)

### TABLE ATTENUATION

Mode	Submode/Image Quality	Doserate (mGy/min)	Table attenuation %	Absorber
C-arm at 0°	Normal	5.601	2.08	2 mmCu
C-arm at 90°	Normal	5.720		

Measurement of doserate in fluoroscopy for the same mode and field size

## MAXIMUM DOSERATE ASSESSMENT

Chamber to focus distance (cm.) 41.6 cm.

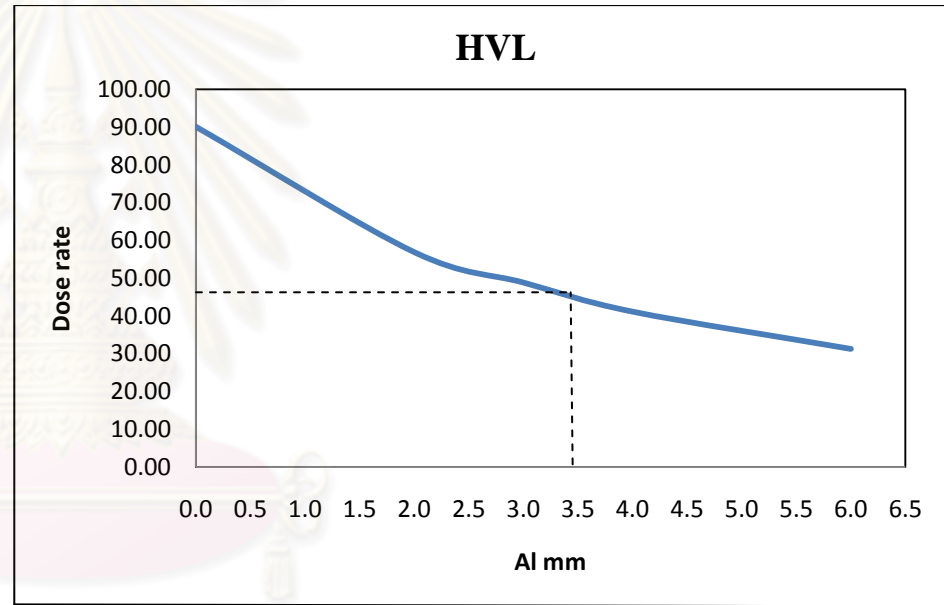
Mode	Submode/ Image quality	Field size (cm)	kV	mA	Dose rate (mGy/min)
Fluoro 1	Normal	40	109.0	2.0	59.28
		28	110.0	2.7	77.70
		20	110.0	4.0	122.04
		14	110.0	4.0	123.06
Fluoro 2	Normal	40	92.0	4.8	104.22
		28	99.0	4.6	110.94
		20	110.0	4.0	122.04
		14	110.0	4.0	121.32
Fluoro 3	Normal	40	92.0	4.8	65.40
		28	99.0	4.5	70.98
		20	110.0	4.0	78.30
		14	110.0	4.0	76.74
Turbo	Normal	40	110.0	4.0	120.36
		28	110.0	4.0	119.64
		20	110.0	4.0	116.40
		14	110.0	4.0	116.94

\*Measure dose rate for all modes and FOVs, dosimeter on the table and table at the lowest position Absorber: 2 mm of lead on the image intensifier (or equivalent attenuation with a folded lead apron)



## HALF VALUE LAYER ASSESSMENT

Al attenuator (mm)	Submode/ Image quality	Dose rate (mGy/min)	HVL (mmAl)
0.0	Normal	90.12	3.49
2.0		56.91	
3.0		48.86	
4.0		41.15	
6.0		31.28	
-	-	-	



Make measurement in fluoroscopy mode, add attenuator (copper sheets) on I.I. to drive kV to 80 kV

ศูนย์วิจัยกัมพูชา  
จุฬาลงกรณ์มหาวิทยาลัย

## IMAGE QUALITY ASSESSMENT

Resolution should be assessed in the usual illumination conditions and from the operator's position.

Leeds Test placed on Image flat-panel detector entrance surface with grid.

High contrast resolution should have strip pattern at about 45° in respect to raster lines (no absorbers; kv: 40-60).

All modes (fluoroscopy and image acquisition) and image qualities and FOVs.

Monitor Focus-Intensifier detector 100 cm.

Mode	Submode/ Image quality	Focus (S/L)	Automatic added filtration (mm Cu)	Field size (cm)	kV	mA	ms	Live image	
								High contrast resolution,lp/mm	Low contrast % contrast
Fluoro1	Continuous	L	0.0	40	63.0	0.4		0.63	0.049
				28	65.0	0.5		0.80	0.075
				20	69.0	0.6		1.00	0.067
				14	73.0	0.7		1.40	0.053
Single shot		L		40	77.0	1.8		0.80	0.045
				28	77.0	2.1		1.00	0.032
				20	77.0	4.3		1.40	0.032
				14	77.0	7.3		1.80	0.032

จุฬาลงกรณ์มหาวิทยาลัย

## APPENDIX B

### เอกสารข้อมูลคำอธิบายสำหรับผู้ป่วยที่เข้าร่วมการวิจัย

การวิจัยเรื่อง การศึกษาปริมาณรังสีที่ผู้ป่วย แพทย์และเจ้าหน้าที่ที่ได้รับจากการส่องกล้องตรวจรักษาต่อทางเดินน้ำดีและตับอ่อน

เรียน ผู้เข้าร่วมวิจัยทุกท่าน

ท่านเป็นผู้ได้รับเชิญจากผู้วิจัยให้เข้าร่วมการศึกษาเพื่อวัดปริมาณรังสีที่ผู้ป่วย แพทย์และเจ้าหน้าที่ที่ได้รับจากการส่องกล้องตรวจรักษาต่อทางเดินน้ำดีและตับอ่อน โดยใช้เครื่องแคปมิเตอร์และเครื่องวัดรังสีเทอร์โมลูมิเนสเซนซ์โดสมิเตอร์ ก่อนที่ท่านตกลงเข้าร่วมการศึกษาดังกล่าว ขอเรียนให้ท่านทราบถึงเหตุผลและรายละเอียดของการศึกษาวิจัย ในครั้งนี้

ผู้ป่วย แพทย์และเจ้าหน้าที่ที่ทำการส่องกล้องตรวจรักษาต่อทางเดินน้ำดีและตับอ่อน ในหน่วยเอ็กซเรย์หลอดเลือดและรังสีร่วมรักษา มีความเสี่ยงที่จะได้รับปริมาณรังสีสูงกว่าการตรวจวินิจฉัยโดยทั่วไปในหน่วยงานอื่นๆ ภายในโรงพยาบาล เพราะผู้ป่วย แพทย์และเจ้าหน้าที่

ดังนั้นการศึกษาวิจัยในครั้งนี้ มีวัตถุประสงค์เพื่อ วัดปริมาณรังสีที่ผู้ป่วย แพทย์และเจ้าหน้าที่ได้รับในส่วนต่างๆ ของร่างกาย ต่อการตรวจหรือการรักษาแต่ละครั้งว่าเป็นปริมาณเท่าไร และมีวิธีการลดปริมาณรังสีที่ผู้ป่วย แพทย์และเจ้าหน้าที่ได้รับอย่างไร เพื่อไม่ให้เกินปริมาณรังสีสูงสุดที่สามารถรับได้

เครื่องวัดรังสีเทอร์โมลูมิเนสเซนซ์โดสมิเตอร์ ทำมาจากลิเทียมฟลูออไรด์ซึ่งมีแมกนีเซียมและไททาเนียมเป็นส่วนผสมอยู่ มีขนาดกว้าง 3.2 มิลลิเมตร ยาว 3.2 มิลลิเมตร หนา 0.89 มิลลิเมตร ซึ่งมีขนาดเล็กมากจึงไม่เป็นอุปสรรคในการทำงานของแพทย์และเจ้าหน้าที่ขณะปฏิบัติงาน

เครื่องแคปมิเตอร์ เป็นเครื่องมือที่ใช้วัดปริมาณรังสีที่ออกมาจากหลอดเอ็กซเรย์โดยตรง จะนำแผ่นฟิล์มวางบนเตียงได้ตัวผู้ป่วยบนเตียงเอ็กซเรย์ตรงบริเวณที่รังสีผ่านตัวผู้ป่วย ส่วนหัววัดจะติดอยู่ที่หลอดเอ็กซเรย์โดยเครื่องอ่านค่าจะแยกออกมาต่างหาก ซึ่งอุปกรณ์ชนิดนี้จะไม่รบกวนหรือเป็นอุปสรรคทั้งผู้ป่วย แพทย์และเจ้าหน้าที่ในขณะปฏิบัติงาน

หากท่านตกลงที่จะเข้าร่วมการศึกษานี้ จะมีข้อปฏิบัติร่วมดังต่อไปนี้

- ท่านไม่ต้องเสียค่าใช้จ่ายใดๆทั้งสิ้น นอกจากค่าตรวจรักษาตามปกติ
- ก่อนเริ่มการตรวจในแต่ละครั้ง ผู้วิจัยจะติดตัววัดรังสีเทอร์โมลูมิเนสเซนซ์ ในส่วนต่างๆ ของร่างกาย คือ ตาซ้าย, ต่อมไทรอยด์ข้างในเสื้อตะกั่ว, แขนซ้าย, ขาซ้าย และบริเวณช่องท้องส่วนล่าง และติดแผ่นฟิล์มบนเตียงเอ็กซเรย์ได้ตัวผู้ป่วยตรงบริเวณที่รังสีผ่านตัวผู้ป่วย
- ท่านอาจเกิดการระคายเคืองจากเครื่องมือและอุปกรณ์ที่ใช้ในการคิดเพื่อตรวจวัดรังสีเพียงเล็กน้อย

- หลังจากที่ผู้ป่วย แพทย์และเจ้าหน้าที่ทำการตรวจหรือการรักษาเสร็จ ในแต่ละการตรวจ ผู้วิจัย จะทำการเก็บตัววัดรังสีเทอร์โมลูมิเนสเซนซ์และแผ่นฟิล์มออก เพื่อนำไปอ่านและคำนวณหาปริมาณรังสีที่แพทย์และเจ้าหน้าที่ได้รับในการตรวจครั้งนั้นๆ
- หากเกิดอันตรายใดๆ จากการทำวิจัยดังกล่าวผู้เข้าร่วมวิจัยจะได้รับการรักษาพยาบาลโดยไม่เสียค่าใช้จ่ายใดๆทั้งสิ้น

การเข้าร่วมการศึกษาวิจัยนี้ เป็นไปโดยสมัครใจท่านอาจจะปฏิเสธที่จะเข้าร่วม หรือถอนตัวจากการศึกษาวิจัยนี้ได้ทุกเมื่อ โดยไม่กระทบต่อการให้บริการและการรักษาที่ท่านจะได้รับจากแพทย์และเจ้าหน้าที่หรือผู้ให้บริการท่านอื่นๆ

ประการสำคัญที่ท่านควรทราบ คือ ผลของการศึกษาวิจัยนี้ จะใช้สำหรับวัตถุประสงค์ทางวิชาการเท่านั้น โดยข้อมูลต่างๆของท่านจะถูกเก็บเป็นความลับ โดยจะเปิดเผยข้อมูลเป็นภาพรวมในแง่วิชาการเพื่อความปลอดภัยของผู้ป่วยจากการตรวจวินิจฉัยและรักษาด้วยรังสีเท่านั้น

หากท่านมีปัญหา หรือข้อสงสัยประการใด กรุณาติดต่อ นายวชิรพงศ์ สุวรรณบุญฤทธิ์ โทร 084-917-8866 ซึ่งยินดีให้คำตอบแก่ท่านทุกเมื่อ ขอขอบคุณในความร่วมมือของท่านมา ณ ที่นี้

ศูนย์วิทยทรัพยากร  
จุฬาลงกรณ์มหาวิทยาลัย

## ใบยินยอมเข้าร่วมการวิจัย (Consent form)

การวิจัยเรื่อง การศึกษาปริมาณรังสีที่ผู้ป่วย แพทย์และเจ้าหน้าที่ได้รับจากการส่องกล้องตรวจรักษาต่อทางเดินน้ำดีและตับอ่อน

วันที่ให้คำยินยอม วันที่ ..... เดือน..... พ.ศ.....

ก่อนที่จะลงนามในใบยินยอมให้ทำการวิจัยนี้ ข้าพเจ้าได้รับการอธิบายจากผู้วิจัยถึงวัตถุประสงค์ของการทำวิจัย ระยะเวลาของการทำวิจัย วิธีการวิจัย อันตราย หรืออาการที่อาจเกิดขึ้นจากการทำการวิจัย รวมทั้งประโยชน์ที่จะเกิดขึ้นจากการทำวิจัยอย่างละเอียดและมีความเข้าใจดีแล้ว

ผู้วิจัยรับรองว่าจะตอบคำถามต่างๆ ที่ข้าพเจ้าสงสัยด้วยความเต็มใจ ไม่ปิดบังซ่อนเร้นจนข้าพเจ้าพอใจ

ข้าพเจ้ามีสิทธิที่จะบอกเลิกการเข้าร่วมในโครงการวิจัยนี้เมื่อใดก็ได้ โดยไม่จำเป็นต้องแจ้งเหตุผล และการบอกเลิกการเข้าร่วมวิจัยนี้ จะไม่มีผลต่อการรักษาโรคหรือสิทธิอื่นๆที่ข้าพเจ้าจะพึงได้รับต่อไป

ผู้วิจัยรับรองว่าจะเก็บข้อมูลเฉพาะเกี่ยวกับตัวข้าพเจ้าเป็นความลับ และจะเปิดเผยได้เฉพาะในรูปแบบที่เป็นสรุปผลการวิจัย การเปิดเผยข้อมูลเกี่ยวกับตัวข้าพเจ้าต่อหน่วยงานต่างๆ ที่เกี่ยวข้องกระทำได้เฉพาะกรณีที่ทำเป็น ด้วยเหตุผลทางวิชาการเท่านั้น

ผู้วิจัยรับรองว่าจะไม่เก็บข้อมูลใดๆ ของข้าพเจ้าเพิ่มเติม หลังจากที่ข้าพเจ้าขอยกเลิกการเข้าร่วมโครงการวิจัย

ข้าพเจ้าได้อ่านข้อความข้างต้นแล้ว และมีความเข้าใจดีทุกประการ และได้ลงนามในใบยินยอมนี้ด้วยความเต็มใจ

ศูนย์วิทยุทรัพยากร  
จุฬาลงกรณ์มหาวิทยาลัย

ลงนาม.....ผู้ยินยอม

(.....)

วันที่.....เดือน..... พ.ศ.....

ลงนาม..... พยาน

(.....)

วันที่.....เดือน..... พ.ศ.....

ลงนาม.....ผู้ทำวิจัย

(.....)

วันที่.....เดือน..... พ.ศ.....

## APPENDIX C

CASE RECORD FORM FOR ERCP PROCEDURE

Information		remarks
Date	(D/M/Y)	
Patient No.	xxx	
Procedure	ERCP	
Height (cm)	xx	
Weight (kg)	xx	
Gender	M/F	
Portal film in place?	y/n	
Age	xx	
Initial DAP setting	y/n	
Start time	xx.xx	
Tube voltage (kVp)	xx	
SID (cm)	xx	
Tube current (mA)	xx	
Filtration (mmAl)	xx	
FOV	Mag1,2,3	
Number of frame (f/s)	xx	
Fluoroscopy time (min)	xx.xx	
End time	xx.xx	
Position	Prone/ Lt Lat	
DAP meter reading	xxxx	
Area film (cm <sup>2</sup> )	xxx	
Data collector	xxxxx	



## APPENDIX D

### Report the radiation dose profile survey

Interventional Radiology Unit, Department of Radiology, Naratip Pongprapan Building, Chulalongkorn Memorial Hospital

X-ray Manufacturer: Siemens Polystar Model No.1148902 S/N 2107

Generator Model Polydoros SX II 40×40 cm. Filter 0.1 mmCu.

#### The left lateral position

1. The left side of the patient was 94.3  $\mu\text{Gy/hr}$  at 0.6 meter from the x-ray tube
2. The left side of the patient was 229.3  $\mu\text{Gy/hr}$  at 0.6 meter from the x-ray tube
3. The right side of the patient was 313.3  $\mu\text{Gy/hr}$  at 0.5 meter from the x-ray tube
4. The right side of the patient was 650  $\mu\text{Gy/hr}$  at 0.6 meter from the x-ray tube
5. The table end was 74.8  $\mu\text{Gy/hr}$  at 1.3 meter from the x-ray tube

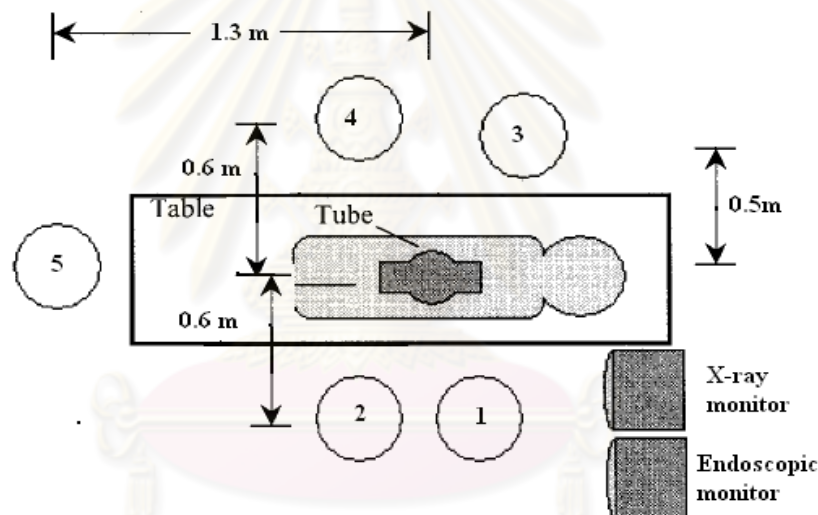
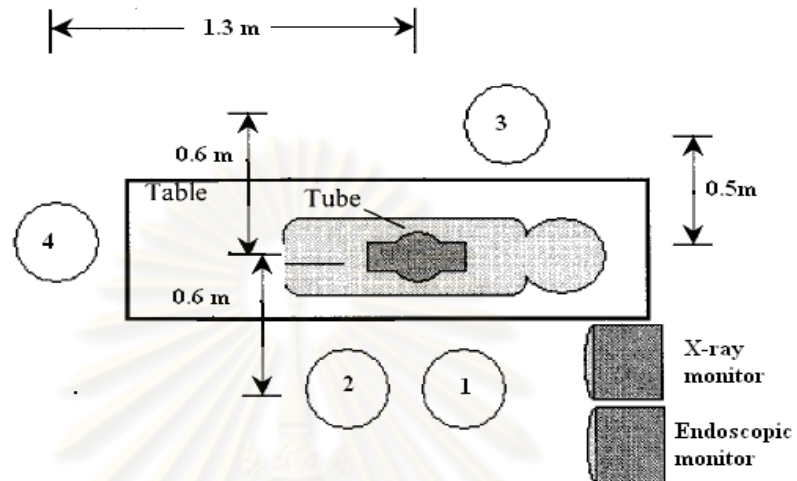


Figure I. Medical staff positions at patient left lateral position

### The prone position

1. The left side of the patient was 1.0 mGy/hr at 0.6 meter from the x-ray tube
2. The left side of the patient was 1.0 mGy/hr at 0.6 meter from the x-ray tube
3. The right side of the patient was 374.3  $\mu$ Gy/hr at 0.5 meter from the x-ray tube
4. The table end was 40.3  $\mu$ Gy/hr at 1.3 meter from the x-ray tube



**Figure II.** Medical staff positions at patient prone lateral position

Conclusion: The radiation dose to medical staff was not exceed the dose limit

## รายงานการวัดอัตราการแผ่รังสีจากเครื่อง **Radiographic Fluoroscopic system**

ตึกนราธิปพงษ์ประพันธ์ ฝ้ายรังสีวิทยา โรงพยาบาลจุฬาลงกรณ์ สภากาชาดไทย

ผลิตภัณฑ์ ซีเมนต์ รุ่น Polystar Model No.1148902 S/N 2107

Generator Model Polydoros SX II ขนาด 40×40 cm. Filter 0.1 mmCu.

การแผ่รังสีรอบๆเตียงผู้ป่วย ของเครื่อง X-ray โดยผู้ป่วยนอนตะแคงซ้ายเป็นดังนี้

1. ที่ด้านซ้ายของผู้ป่วย 94.3 ไมโครเกรย์/ชม. ที่ระยะ 0.6 เมตร จากหลอด X-ray
2. ที่ด้านซ้ายของผู้ป่วย 229.3 ไมโครเกรย์/ชม. ที่ระยะ 0.6 เมตร จากหลอด X-ray
3. ที่ด้านขวาของผู้ป่วย 313.3 ไมโครเกรย์/ชม. ที่ระยะ 0.5 เมตร จากหลอด X-ray
4. ที่ด้านขวาของผู้ป่วย 650 ไมโครเกรย์/ชม. ที่ระยะ 0.6 เมตร จากหลอด X-ray
5. ที่บริเวณปลายเตียง 74.8 ไมโครเกรย์/ชม. ที่ระยะ 1.3 เมตร จากหลอด X-ray

การแผ่รังสีรอบๆเตียงผู้ป่วย ของเครื่อง X-ray โดยผู้ป่วยนอนคว่ำเป็นดังนี้

1. ที่ด้านซ้ายของผู้ป่วย 1.0 มิลลิเกรย์/ชม. ที่ระยะ 0.6 เมตร จากหลอด X-ray
2. ที่ด้านซ้ายของผู้ป่วย 1.0 มิลลิเกรย์/ชม. ที่ระยะ 0.6 เมตร จากหลอด X-ray
3. ที่ด้านขวาของผู้ป่วย 374.3 ไมโครเกรย์/ชม. ที่ระยะ 0.5 เมตร จากหลอด X-ray
4. ที่บริเวณปลายเตียง 40.3 ไมโครเกรย์/ชม. ที่ระยะ 1.3 เมตร จากหลอด X-ray

สรุป ปริมาณรังสีที่แพทย์และพยาบาลได้รับระหว่างการปฏิบัติงานอยู่ในเกณฑ์ที่ปลอดภัย

ศูนย์วิทยุทรัพยากร  
จุฬาลงกรณ์มหาวิทยาลัย

## VITAE

**Name:** Mr. Wachirapong Suwanboonrit

**Sex:** Male

**Date of birth:** April 29, 1982

**Place of birth:** Suphanburi, Thailand

**Home Address:** 111/134 M.3 Mooban Rung-Arun T. Plaibang A. Bangkruay,  
Nonthaburi, Thailand 11130  
Tel. 084-917-8866

**Qualification:** Bachelor of Science (Medical Instrumentation),  
King Mongkut's Institute of Technology North Bangkok, 2005

**Job experiences:** Medical Technician of Department of Therapeutic Radiology and  
Oncology, King Chulalongkorn Memorial Hospital, Thai Red  
Cross Society for 2 years.  
Medical Technology Technician of Asset Management Systems  
(Thailand) Co. LTD. Society for 10 months.



ศูนย์วิทยทรัพยากร  
จุฬาลงกรณ์มหาวิทยาลัย